

\ A PREDICTIVE ADAPTIVE DELTA MODULATOR /

by

Yuh-tai, Ju

Thesis submitted to the Graduate Faculty of the
Virginia Polytechnic Institute and State University
in partial fulfillment of the requirement for the degree of
MASTER OF SCIENCE
in
Electrical Engineering

APPROVED:

~~Dr. H. F. VanLandingham~~, Chairman

Dr. I. M. Besieris

Dr. R. A. Thompson

December, 1977

Blacksburg, Virginia

ACKNOWLEDGEMENT

LM/MRS 6/7/77

I wish to express my appreciation and thanks to my graduate committee: Dr. Richard A. Thompson, Dr. Ioannis M. Besieris and Dr. Hugh F. VanLandingham. Special thanks are extended to Dr. Hugh F. VanLandingham for his guidance, suggestions and a great deal of incalculable assistance in this thesis.

Thanks also go to Virginia Polytechnic Institute and State University, the Department of Electrical Engineering and Dr. William A. Blackwell, the head of the department, for their financial assistance and encouragement during my studies at this university.

TABLE OF CONTENTS

	Page
ACKNOWLEDGEMENT	ii
LIST OF FIGURES	iv
CHAPTER 1 INTROUDCUCTION	1
CHAPTER 2 AN ADAPTIVE DELTA MODULATOR	6
CHAPTER 3 A PREDICTIVE ADAPTIVE DELTA MODULATOR	13
CHAPTER 4 DISCUSSION OF THE NYQUIST INTERVAL	18
CHAPTER 5 COMPARISON BETWEEN DIFFERENT TYPES OF ADAPTIVE DELTA MODULATORS	26
CHAPTER 6 RESULTS AND RECOMMENDATIONS	29
BIBLIOGRAPHY	52
APPENDIX	53
VITA	64
ABSTRACT	

LIST OF FIGURES

<u>Figure</u>		<u>Page</u>
1-1	Block Diagram of Non-predictive Adaptive Delta Modulator	3
1-2	Block Diagram of Predictive Adaptive Delta Modulator	4
2-1	Block Diagram of a Bi-state ADM	7
2-2	Results of Example 1	9
2-3	Results of Example 2	9
2-4	Block Diagram of a Tri-state ADM	10
2-5	Results of Example 3	12
3-2.1	Block Diagram for the Operation of A Predictive Adaptive Delta Modulator	14
4-1	A Discrete Time System	19
4-3.1	$G_1(w)$	22
4-3.2	$G_2(w)$	22
4-4.1	The Operation of the Encoding of an Unknown Input Signal with Highly Correlated Statistics	24
6-1.1	Mean Error Versus ϕ	31
6-2.1	Type 1 Encoding with Bi-state Quantizer	32
6-2.2	Type 2 Encoding with Bi-state Quantizer	33
6-2.3	Type 3 Encoding with Bi-state Quantizer	34
6-2.4	Type 1 Encoding with Tri-state Quantizer	36
6-2.5	Type 2 Encoding with Tri-state Quantizer	37
6-2.6	Type 3 Encoding with Tri-state Quantizer	38
6-2.7	Type 1 Encoding with Bi-state Quantizer	39

LIST OF FIGURES (Continued)

<u>Figure</u>	<u>Page</u>
6-2.8 Type 2 Encoding with Bi-state Quantizer	40
6-2.9 Type 3 Encoding with Bi-state Quantizer	41
6-2.10 Type 1 Encoding with Tri-state Quantizer	42
6-2.11 Type 2 Encoding with Tri-state Quantizer	43
6-2.12 Type 3 Encoding with Tri-state Quantizer	44
6-2.13 Type 1 Encoding with Bi-state Quantizer	45
6-2.14 Type 2 Encoding with Bi-state Quantizer	46
6-2.15 Type 3 Encoding with Bi-state Quantizer	47
6-2.16 Type 1 Encoding with Tri-state Quantizer	48
6-2.17 Type 2 Encoding with Tri-state Quantizer	49
6-2.18 Type 3 Encoding with Tri-state Quantizer	50

Chapter 1

Introduction

In recent years, the demand for point to point communication and in particular, long distance telephone calls, have increased very rapidly. Overseas calls have multiplied tenfold in the past fifteen years and still there appears to be no end to this demand.

Delta modulation has been known for almost three decades (Ref. 8). Delta modulation possesses two main assets: namely, that of being digital in nature and that of not requiring complex equipment. This latter asset promises to alleviate overcrowded transmission facilities. Scientists have predicted that the satellite links and microwave relay stations that presently interconnect major cities of the world will in the future transmit human speech in the form of digital bits rather than voice waveforms.

To answer the question of why scientists make this prediction when analog waveforms are more prevalent today, we must recognize that digital signals are relatively insensitive to noise, cross talk and distortion. Moreover, because of recent technology, both economic considerations and intersystem compatibility arguments favor the use of digital communication in the future.

In this thesis, only digital signals are considered rather than signals which are encoded in an analog fashion before transmission.

1-1. Non-predictive Adaptive Delta Modulator

The standard structure for a Non-predictive Adaptive Delta Modulator is illustrated in Fig. 1-1.

With the aid of the well-known Kalman Filter algorithm some of the system noise can be filtered out. The quantizer can be a bi-state or tri-state quantizer. Later on, comparisons between the bi-state and tri-state quantizer, and between systems with and without Kalman Filter encodings will be discussed.

1-2. Predictive Adaptive Delta Modulator

The structure for a Predictive Adaptive Delta Modulator is shown in Fig. 1-2.

Again, comparisons between the bi-state and tri-state quantizers, and between systems with and without Kalman Filter encodings will be discussed.

It is well known that delta modulation suffers from two intrinsic errors. The first one is slope-overload which happens whenever the incoming signal slope is too large. To improve this slope-overload problem, an adaptive logic circuit is used which would catch up with the steep slope very quickly. However, it also suffers from another type of error which is called idle noise. Idle noise happens whenever the incoming signal slope is nearly zero and the corresponding DM signal oscillates about the actual signal. There are several ways to improve this type of degradation. For example, by reducing the control gain and decreasing the sampling intervals, i.e. increasing the

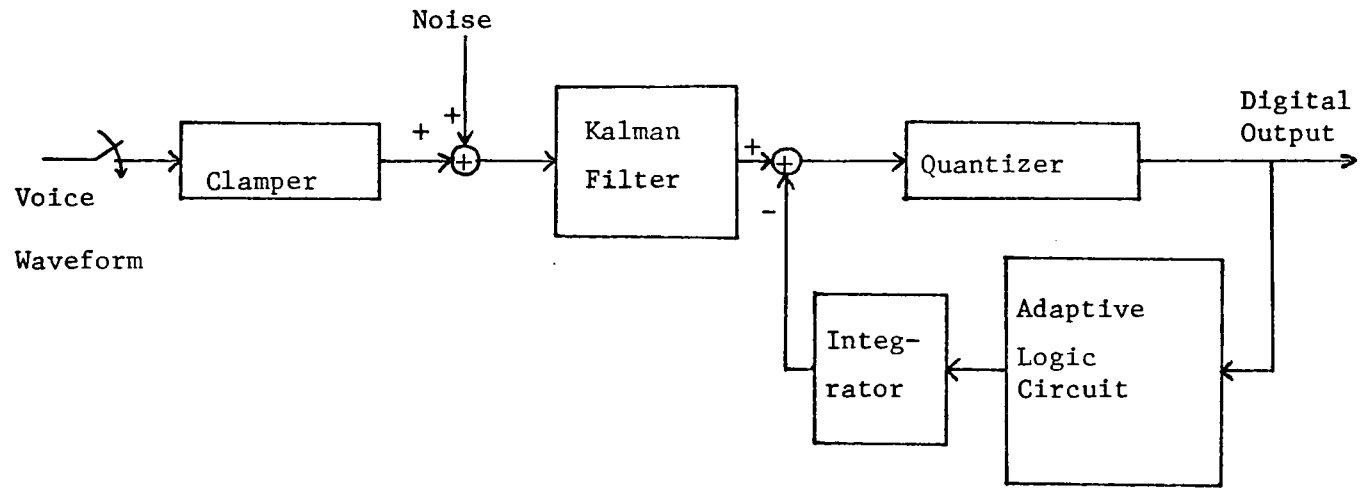


Figure 1-1. Block Diagram of Non-predictive Adaptive Delta Modulator

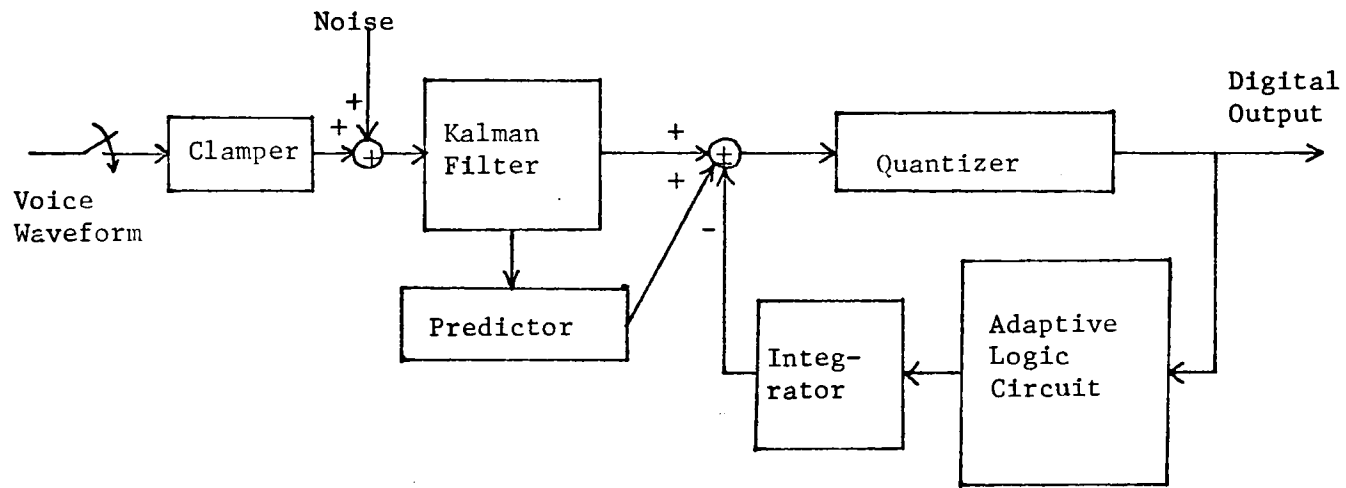


Figure 1-2. Block Diagram of Predictive Adaptive Delta Modulator

sampling frequency. Therefore, the compromise between the control gain and the sampling frequency will dominate the usage of the delta modulator. However, in this thesis, it was found that the tri-state quantizer can help in reducing this idle noise problem and makes the output closely follow the original waveform. Finally an investigation of the sampling frequency from the Nyquist theory's point of view will be discussed.

Chapter 2

AN ADAPTIVE DELTA MODULATOR (ADM)

Early work on delta modulation (DM) was restricted to a fixed-step-size delta modulator. In order to control the total quantizing noise, the fixed-step-size modulator had to utilize a higher sampling rate than that required of an adaptive delta modulator. However, in recent years, the use of a time-varying, i.e. adaptive step size algorithm in the feedback loop has been investigated and emphasized. This adaptive or companding mechanism can provide considerable improvement in efficiency and therefore a better performance. This chapter is to present an approach described by Taub and Schilling (Ref.1) for the implementation of an adaptive delta modulator.

The algorithm for the bi-state logic circuit is quite simple and is cited below.

If input digits OP_k , as shown in Fig. 2-1, alternate between 1 and -1, $AK=1$; if a sequence of N positive or N negative pulses occurs, AK increases by N ; if after a sequence of N pulses, the parity changes, AK decreases by 2.

Fig. 2-1 is a functional block diagram which indicates the signal processing operations when the quantizer being used is a bi-state quantizer.

The binary-level quantizer determines the polarity of each output pulse according to the state of a single bit of the integrator. The varying step size logic circuit provides a digital representation of

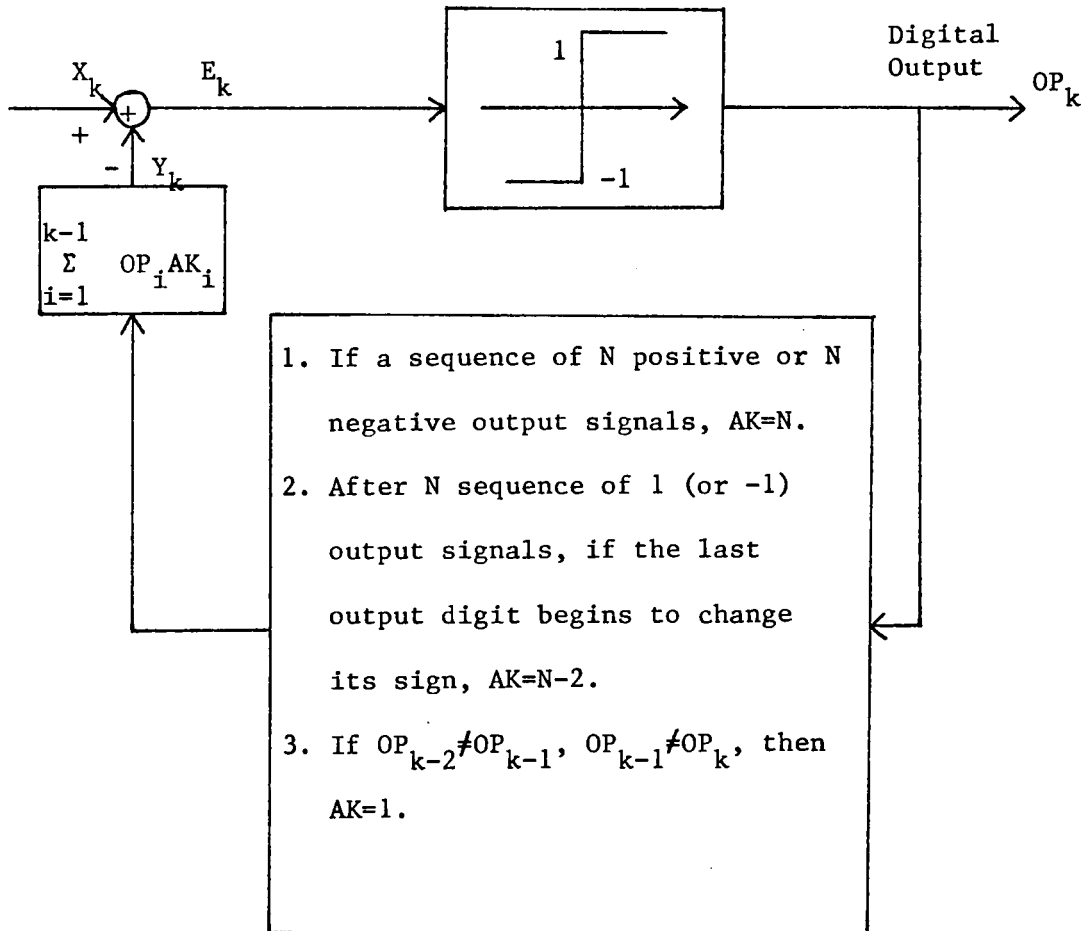


Figure 2-1. Block Diagram of a bi-state ADM.

the current step size. Two typical responses are shown below.

Example 1. If the input signal X_k is kept constant, such that $X_k=12$ for all k . Then the output sequence Y_k is shown in Fig. 2-2.

Example 2. If the input signal X_k is kept constant, such that $X_k=11$ for all k , then the output Y_k is shown in Fig. 2-3.

Fig. 2-4 is a functional block diagram of using a tri-state quantizer.

This tri-state quantizer can do a better job in reducing the idle noise than the bi-state quantizer. The algorithm for its logic circuit is modified a little bit and described below.

If input digits $OP_k=0$, $AK=2$; if OP_k alternate among 0,1 and -1, $AK=1$; if a sequence of N positive or N negative pulses occurs, AK increases by N ; if after a sequence of N pulses, the output digit varies, AK decreases by 1.

Concerning the receiver (or decoder), the feedback portion of the ADM can reconstruct a rather similar signal to the input signal and can therefore serve as a receiver. Of course, efforts should be made to reduce the quantizing error E_k as much as possible. The improvement of the tri-state quantizer in reducing the idle noise is illustrated in Example 3.

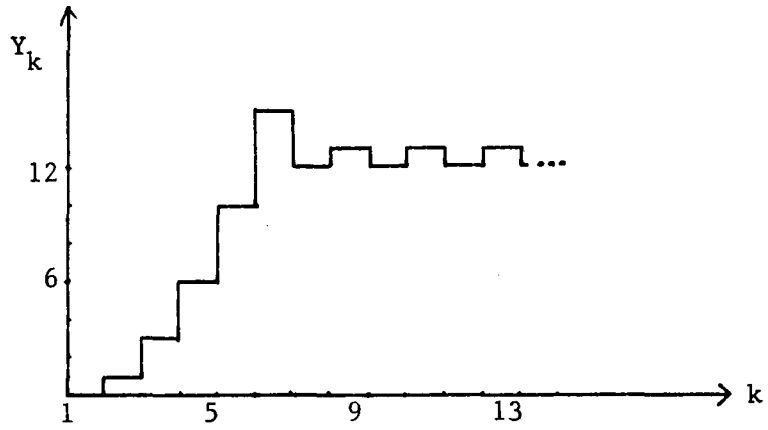


Figure 2-2. Results of Example 1.

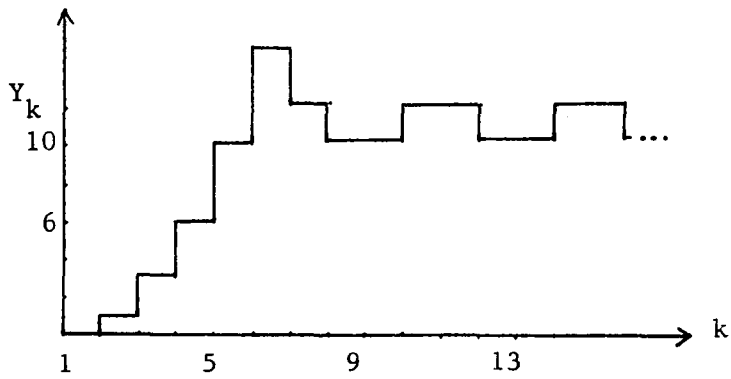


Figure 2-3. Results of Example 2.

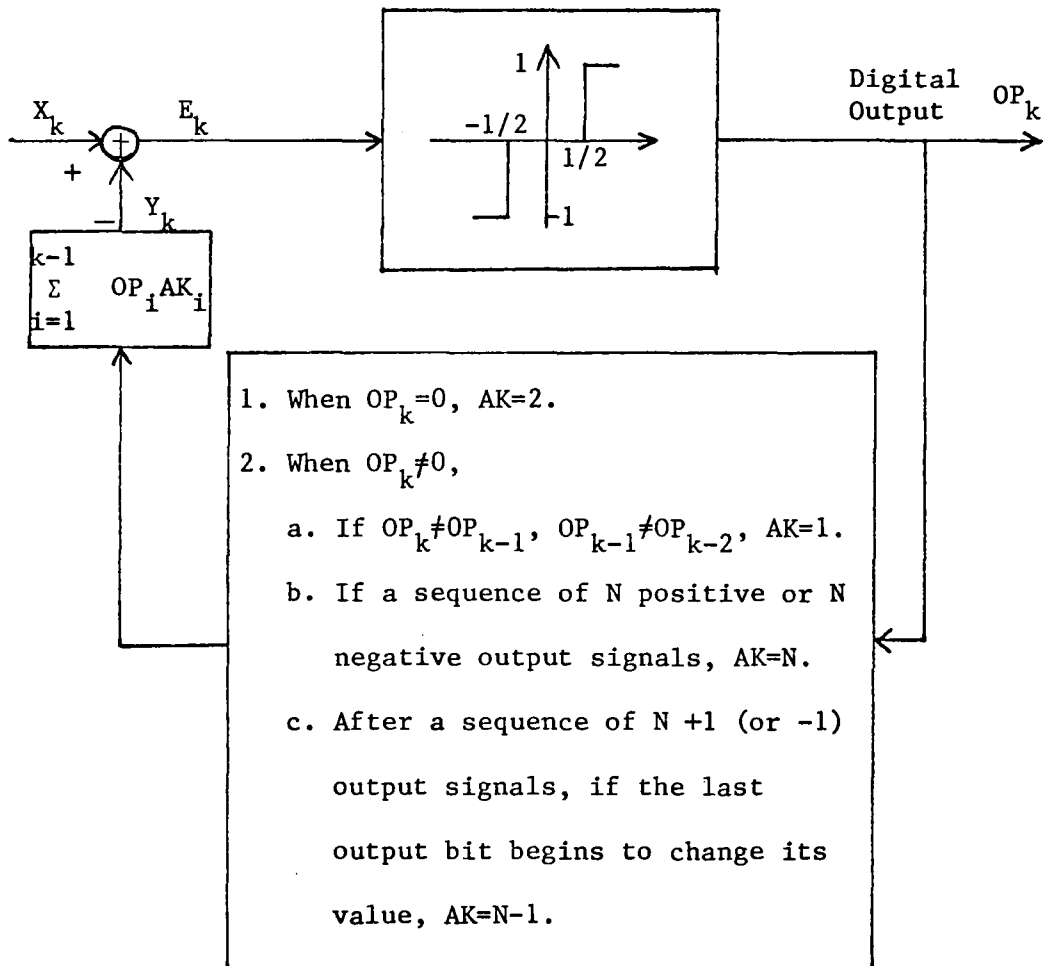


Figure 2-4. Block Diagram of A Tri-state ADM

Example 3. If the input signal $X_k=12$ for $k=1,2,3, \dots, 100$, then $X_k=8$ for $k=101,102,103, \dots$, the output Y_k is shown in Fig. 2-5.

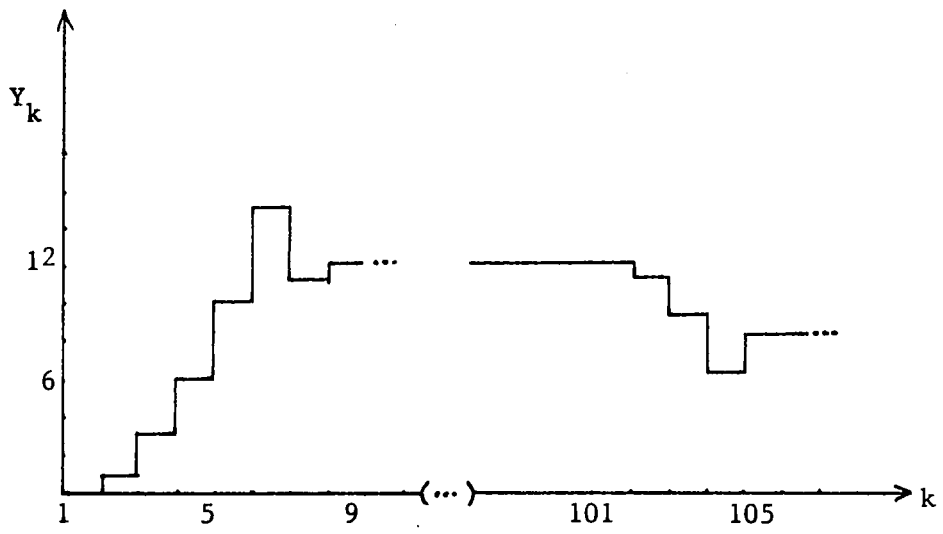


Figure 2-5. Results of Example 3.

Chapter 3

A PREDICTIVE ADAPTIVE DELTA MODULATOR

3-1. Predictor (See Fig. 3-2.1)

For a differentiable time function, a Taylor series is a good way to approximate the function values in the neighborhood of a given time. Truncating the higher order terms will not significantly increase the error of the approximation, especially when the time difference is very small.

$$\bar{X}_k = \hat{X}_{k+1} = \hat{X}_k + \Delta \hat{X}_k + \frac{\Delta^2 \hat{X}_k}{2} + \frac{\Delta^3 \hat{X}_k}{3!} + \dots \quad (3-1)$$

$$\cong \hat{X}_k + \Delta \hat{X}_k + \frac{\Delta^2 \hat{X}_k}{2}$$

$$= [1, 1, 1/2] \cdot \begin{bmatrix} \hat{X}_k \\ \Delta \hat{X}_k \\ \Delta^2 \hat{X}_k \end{bmatrix}$$

$$= \alpha \begin{bmatrix} \hat{X}_k \\ \Delta \hat{X}_k \\ \Delta^2 \hat{X}_k \end{bmatrix} = \alpha \hat{X}_k \quad (3-2)$$

where $\alpha = [1, 1, 1/2]$, $\hat{X}_k = \begin{bmatrix} \hat{X}_k \\ \Delta \hat{X}_k \\ \Delta^2 \hat{X}_k \end{bmatrix}$.

3-2. Kalman Filter

In 1960, Kalman and others advanced an optimal recursive filter technique, known as the Kalman filter, based on state space, time domain formulations, which is ideally suited for digital computer

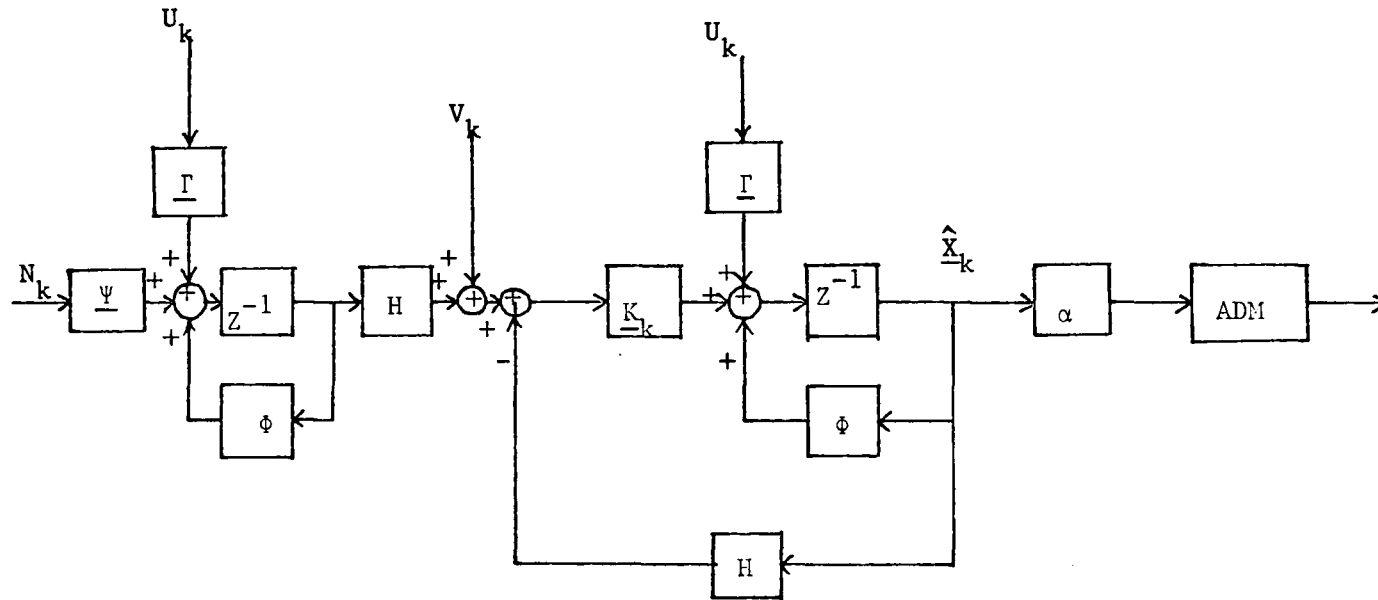


Figure 3-2.1. Block Diagram for the Operation of A
 Predictive Adaptive Delta Modulator.

implementations. In short, the Kalman Filter is a recursive solution that processes external measurements to deduce a minimum error estimate of the state of a system. Therefore, for a highly correlated signal which is disturbed by additive noise when transmitted through a channel, the Kalman Filter can be used to estimate the signal. The requirements for designing the Kalman Filter are system and measurement dynamics with assumed statistics of system noises and measurement errors and initial conditions which generate the signal statistics. This signal and the system state are estimated in the sense of minimum variance error by the Kalman algorithm.

Let
$$\underline{X}_k = \begin{bmatrix} X_k \\ \Delta X_k \\ \Delta^2 X_k \end{bmatrix} = \begin{bmatrix} X_k \\ X_k - X_{k-1} \\ X_{k+1} - 2X_k + X_{k-1} \end{bmatrix} = \begin{bmatrix} L_k \\ M_k \\ J_k \end{bmatrix} \quad \text{for all } k,$$

$$\underline{X}_{k+1} = \begin{bmatrix} X_{k+1} \\ \Delta X_{k+1} \\ \Delta^2 X_{k+1} \end{bmatrix} = \begin{bmatrix} X_{k+1} \\ X_{k+1} - X_k \\ X_{k+1} - 2X_k + X_{k-1} \end{bmatrix} = \begin{bmatrix} L_k \\ M_k \\ J_k \end{bmatrix}$$

For
$$X_{k+1} = \phi X_k + \psi N_k + U_k$$

$$Z_k = X_k + V_k \quad \text{model}$$

with initial condition $X_0 \sim N(m, P_\alpha)$,

$$L_{k+1} = X_{k+1} = \phi X_k + \psi N_k + U_k$$

$$= \phi L_k + \psi N_k + U_k$$

$$M_{k+1} = X_{k+1} - X_k = \phi L_k + \psi N_k + U_k - L_k$$

$$= (\phi - 1)L_k + \psi N_k + U_k$$

$$J_{k+1} = (X_{k+1} - X_k) - (X_k - X_{k-1})$$

$$= (\phi - 1)L_k + \psi N_k + U_k - M_k$$

$$= (\phi - 1)L_k - M_k + \psi N_k + U_k$$

$$\begin{bmatrix} L_{k+1} \\ M_{k+1} \\ J_{k+1} \end{bmatrix} = \begin{bmatrix} \phi, & 0, & 0 \\ \phi - 1, & 0, & 0 \\ \phi - 1, & -1, & 0 \end{bmatrix} \cdot \begin{bmatrix} L_k \\ M_k \\ J_k \end{bmatrix} + \begin{bmatrix} \psi \\ \psi \\ \psi \end{bmatrix} N_k + \begin{bmatrix} 1 \\ 1 \\ 1 \end{bmatrix} U_k \quad (3-3)$$

$$Z_k = [1, 0, 0] \cdot \begin{bmatrix} L_k \\ M_k \\ J_k \end{bmatrix} + V_k \quad (3-4)$$

By defining

$$\Phi = \begin{bmatrix} \phi, & 0, & 0 \\ \phi - 1, & 0, & 0 \\ \phi - 1, & -1, & 0 \end{bmatrix}$$

$$\Psi = \begin{bmatrix} \psi \\ \psi \\ \psi \end{bmatrix}$$

$$\Gamma = \begin{bmatrix} 1 \\ 1 \\ 1 \end{bmatrix}$$

$$H = [1, 0, 0]$$

Then the state equations can be simplified to a more compact one.

$$\underline{X}_{k+1} = \Phi \underline{X}_k + \Psi N_k + \Gamma U_k \quad (3-5)$$

$$Z_k = H \underline{X}_k + V_k \quad (3-6)$$

From data Z_k a Kalman Filter can be used to estimate X_{k+1} .

$$\hat{X}_{k+1} = \Phi \hat{X}_k + \Gamma U_k + K_k [Z_k - H \hat{X}_k] \quad (3-7)$$

$$K_k = \Phi P_k H^T (H P_k H^T + R)^{-1} \quad (3-8)$$

$$P_{k+1} = [\Phi - K_k H] P_k \Phi^T + \Psi Q \Psi^T \quad (3-9)$$

with initial conditions:

$$\hat{X}(0) = [m, 0, 0]^T$$

$$P_0 = \begin{bmatrix} P_\alpha & 0 & 0 \\ 0 & 1 & 0 \\ 0 & 0 & 1 \end{bmatrix}$$

$$N_k \sim N(0, Q)$$

$$V_k \sim N(0, R).$$

From Eq. 3-2, the estimated state vector could be transformed to a predictive state by the theory of Taylor series approximation which provides a predictive input to the ADM as shown in Fig. 3-2.1.

Chapter 4

DISCUSSION OF THE NYQUIST INTERVAL

The purpose of this chapter is to find a reasonable sampling rate for the input signals to the ADM.

In the late 1920's, H. Nyquist did the pioneering work at Bell Telephone Laboratories on the minimum sampling rate. Since the Nyquist theory deals with continuous time functions, a survey will begin from the continuous time domain.

4-1. Relations between continuous time and discrete time systems

Assume that the system model is given by (See Fig. 4-1)

$$\dot{S}(t) = AS(t) + BN''(t), \quad \text{where } A, B \text{ are constants.}$$

Solving this equation,

$$S(t) = e^{At} S(0) + \int_0^t e^{A(t-\tau)} N''(\tau) d\tau \cdot B$$

$$S((n+1)T) = e^{AT} (e^{nAT} S(0) + \int_0^{nT} e^{A(nT-\tau)} N''(\tau) d\tau \cdot B) + D$$

$$= e^{AT} S(nT) + \int_0^T e^{A\lambda} d\lambda \cdot B \cdot N''(nT)$$

with $\lambda = (n+1)T - \tau$, $D = \int_0^T e^{A\lambda} d\lambda \cdot B \cdot N''(nT)$.

Define:

$$\phi = e^{AT}, \quad \psi = \int_0^T e^{A\lambda} d\lambda \cdot B$$

$$S((n+1)T) = \phi S(nT) + \psi N''(nT) \tag{4-1}$$

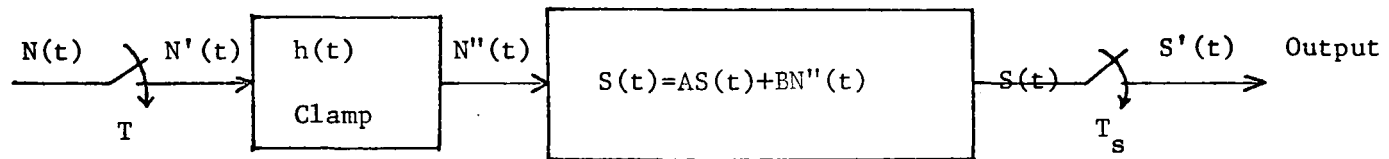


Figure 4-1. A Discrete Time System.

4-2. The transfer function of the discrete time system in Fig. 4-1

4-2.1 Transfer function of a clamp:

$$h(t) = u(t) - u(t-T), \text{ where } u(t) \text{ is unit step function.}$$

The Fourier transform of $h(t)$ is

$$\begin{aligned} H(j\omega) &= 1/j\omega - e^{-j\omega T}/j\omega \\ &= (1 - e^{-j\omega T})/j\omega \end{aligned} \quad (4-2)$$

4-2.3 Transfer function of the system model:

$$\dot{S}(t) = AS(t) + BN''(t)$$

Its transfer function is

$$H_s(j\omega) = \frac{B}{j\omega - A} \quad (4-3)$$

4-2.3 Power spectrum of the input of the clamp.

Assuming that $N''(k)$ is Gaussian, zero mean and statistically independent for different k 's, its Fourier transform is given by

$$N''(\omega) = \sum_{-\infty}^{\infty} N(nT) e^{-j\omega nT}$$

Let $S_n(\omega)$ denotes the power spectrum of $N'(t)$. It is equal to

$$\begin{aligned} \lim_{2NT \rightarrow \infty} \frac{E[N'(\omega) \cdot N'(\omega)]}{2NT} &= \lim_{2NT \rightarrow \infty} \frac{E\left[\sum_{-\infty}^{\infty} N(nT) e^{-j\omega nT} \cdot \sum_{-\infty}^{\infty} N(nT) e^{+j\omega nT}\right]}{2NT} \\ &= 2 \lim_{NT \rightarrow \infty} \frac{E\left[\sum_{-\infty}^{\infty} N^2(nT)\right]}{2NT} \\ &= \lim_{2NT \rightarrow \infty} \frac{2N \cdot \sigma^2}{2NT} \\ &= \sigma^2/T \end{aligned} \quad (4-4)$$

4-2.4 Power spectrum of the output of the system model:

$$\text{Power spectrum of } S(t) = S_s(\omega)$$

$$\begin{aligned}
&= |H_s(j\omega)|^2 \cdot |H(j\omega)|^2 S_{n_r}(\omega) \\
&= \frac{B^2 \sigma^2 T}{A^2 + \omega^2} \cdot \frac{|1 - e^{-j\omega T}|^2}{\omega^2} \\
&= \frac{B^2 \sigma^2 T}{A^2 + \omega^2} \cdot \frac{\sin^2(\omega T/2)}{(\omega T/2)^2} \tag{4-5}
\end{aligned}$$

4-3. Investigation of the Nyquist Interval

The equation of 4-5 is a product of two functions in the frequency (ω) domain. One way to examine it is to discuss each ω -function separately and then combine the results together.

4-3.1 Functional behavior of $G_1(\omega)$:

$$\text{Let } G_1(\omega) = \frac{1}{A^2 + \omega^2}$$

The 3 dB point for the above equation is shown in Fig. 4-3.1.

Picking $\omega_0 = 5|A|$,

$$10 \cdot \log \frac{G_1(0)}{G_1(\omega_0)} = 10 \cdot \log(26) > 14 \text{ dB.}$$

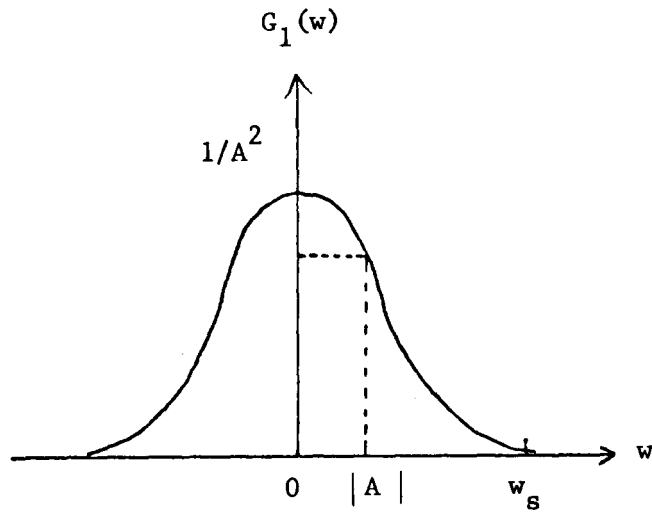
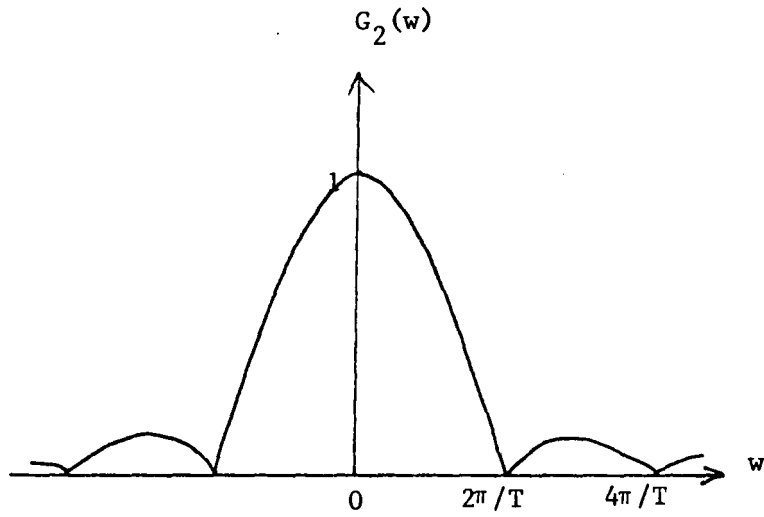
it means $G_1(\omega)$ will be very small in comparison with $G_1(0)$ when $\omega \gg 5|A|$.

4-3.2 Functional behavior of $G_2(\omega)$:

Let $G_2(\omega) = \text{Sa}^2(\omega T/2)$. Its curve is shown in Fig. 4-3.2.

$$10 \cdot \log \frac{G_2(0)}{G_2(2.86\pi/T)} > 13 \text{ dB.}$$

It means that $G_2(2.86\pi/T)$, which is the maximum value of the second

Figure 4-3.1. $G_1(w)$.Figure 4-3.2. $G_2(w)$.

lobe, will be very small in comparison with $G_2(0)$.

4-3.3 Functional behavior of $S_s(w)$:

Since $G_1(w)$ will be negligible when $w > 5|A|$, $G_2(w)$ will also be negligible when $w > 2.86\pi/T$. By the Nyquist theorem, $G_1(w)$ can take the minimum sampling angular frequency of $10|A|$ and $G_2(w)$ can have a minimum sampling angular frequency of $5.72\pi/T$. Now, the equation 4-5 is the product of $G_1(w)$ and $G_2(w)$; therefore, $S_s(w_s)$ will have a 27 dB cut off angular frequency, if $w_s = 10|A|$ and $w_s = 5.72\pi/T$.

In the above case, the discussion is concentrated in a special system model which was generated from a noise input. In section 4-4, the discussion will be centered on unknown input signals which are highly correlated.

4-3.4 For the stability of the system model, $A < 0$ is necessary.

4-4. Nyquist sampling frequency for unknown input signals (See Fig. 4-4.1)

Assuming that the noise N_k is a white, Gaussian distributed, zero mean sequence with variance σ^2 , and that the input signals S_k are highly correlated, $R_s(\tau) = Ke^{-a|\tau|}$, with $K > 0$, $a > 0$; S_k and N_k are statistically independent, then

$$R_s(\tau) = Ke^{-a|\tau|} \quad (4-6)$$

Take Fourier transform of $R_s(\tau)$,

$$S_s(w) = K \frac{2a}{a^2 + w^2} \quad (4-7)$$

Let

$$10 \cdot \log \frac{S_s(0)}{S_s(w)} = 10 \log \left(\frac{a^2 + w_0^2}{a^2} \right) > 20 \text{ dB}$$

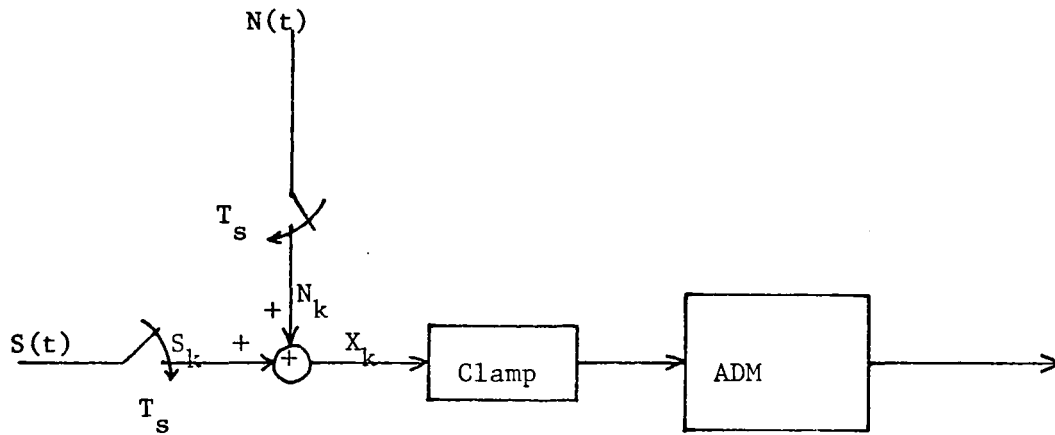


Figure 4-4.1. The Operation of the Encoding of an Unknown
Input Signals with Highly Correlated Statistics.

$$\frac{a^2 + w_0^2}{a^2} \geq 100, \quad w_0 \geq 99a \quad (4-8)$$

From eq. 4-8, a reasonable sampling frequency $w_s = 19.9a$ is chosen in order to reduce that of the crossed tail. a is the parameter of the autocorrelation function $R_s(\tau)$. In eq. 4-6, $1/a$ can be recognized easily as that of the life time of the correlation function $R_s(\tau)$ of the input signals S_k .

Chapter 5

COMPARISON BETWEEN DIFFERENT TYPES OF ADAPTIVE DELTA MODULATORS

An example will be given in this chapter in order to illustrate the operations of different types of adaptive delta modulators.

5-1. Generation of a highly correlated, zero mean, Gaussian signal

If $S_{k+1} = \phi S_k + \psi N_k$, for $k=1,2,3,\dots$

and $R_n = E[S_{k+n} \cdot S_k] = Ke^{-nT/a}$

where ϕ, ψ, K, a are parameters, $K > 0, a > 0, N_k \sim N(0, \sigma^2)$, N_k and S_k are statistically independent and T is the time interval,

then $E[S_{k+1}] = \phi E[S_k] + \psi E[N_k] = \phi E[S_k] = 0$.

$$\begin{aligned} E[S_{k+1}^2] &= E[(\phi S_k + \psi N_k) \cdot (\phi S_k + \psi N_k)] \\ &= \phi^2 E[S_k^2] + 2\phi\psi E[S_k \cdot N_k] + \psi^2 E[N_k^2] \\ &= \phi^2 \cdot K + \psi^2 \cdot \sigma^2 \\ &= K \end{aligned}$$

$$\begin{aligned} E[S_{k+1} \cdot S_k] &= E[(\phi S_k + \psi N_k) \cdot S_k] \\ &= \phi E[S_k^2] + \psi E[N_k \cdot S_k] \\ &= \phi K \\ &= Ke^{-T/a} \end{aligned}$$

From the above equations,

$$\phi = e^{-T/a}$$

$$\psi = K^{1/2} \cdot (1 - \phi^2) / \sigma$$

By properly adjusting T and a , S_k can be highly correlated signals.

If $K=100, \sigma=1, \phi=0.994, \psi$ could be calculated as $\psi=1.0938$. Since K is the variance of S_k , 68% of the S_k values will lie within $(-10, 10)$ and 96% of the S_k values will lie within $(-20, 20)$, provided that $K=100$.

5-2. Generation of a sinusoidally biased highly correlated test signal

The testing signal used is a pseudo-narrowband signal which is a sinusoidal wave superimposed on a highly correlated zero mean, Gaussian noise.

Therefore, $X_k = S_k + 20 \cdot \sin(\pi/80 \cdot k)$

$$\begin{aligned} X_{k+1} &= S_{k+1} + 20 \cdot \sin(\pi/80 \cdot (k+1)) \\ &= \phi(X_k - 20 \cdot \sin(\pi/80 \cdot k)) + \psi N_k + 20 \cdot \sin(\pi/80 \cdot (k+1)) \\ &= \phi X_k + \psi N_k + U_k \end{aligned}$$

where $U_k = 20 \cdot (\sin(\pi/80 \cdot (k+1)) - \phi \sin(\pi/80 \cdot k))$

$$\underline{X}_{k+1} = \begin{bmatrix} 0.994, & 0 & 0 \\ -0.006, & 0, & 0 \\ -0.006, & -1, & 0 \end{bmatrix} \cdot \underline{X}_k + \begin{bmatrix} 1.0938 \\ 1.0938 \\ 1.0938 \end{bmatrix} N_k + \begin{bmatrix} 1 \\ 1 \\ 1 \end{bmatrix} U_k$$

$$Z_k = [1, 0, 0] \underline{X}_k + V_k$$

with initial conditions;

$$\hat{\underline{X}}_0 = \begin{bmatrix} 0 \\ 0 \\ 0 \end{bmatrix}$$

$$P_0 = \begin{bmatrix} 1, & 0, & 0 \\ 0, & 1, & 0 \\ 0, & 0, & 1 \end{bmatrix}$$

$$V_k \sim N(0, 0.5)$$

$$N_k \sim N(0, 1.0).$$

The results of this example are reviewed in the next chapter.

Chapter 6

RESULTS AND RECOMMENDATIONS

6-1. Results

In this thesis, a study was made of six different types of Adaptive Delta Modulators (ADM). In a typical example, Table 1 shows the estimated mean errors of the various ADMs with the parameter ϕ changing from 0.91 to 0.99. The corresponding curves are shown in Fig. 6-1.1.

If a Kalman Filter is included, noise will be somewhat filtered out, and therefore the tracking is improved. Furthermore, if a predictor is added in, the rate of change of the input signal will help the prediction of the highly correlated input signal and guide a direction for the tracking of the next signal. In the above examples, a good correspondence between the input signal and the tracking signal was found for the predictive adaptive delta modulator and the mean error is therefore greatly reduced.

Fig. 6-2.1 and 6-2.2, taken in conjunction with Fig. 6-2.3, demonstrate the use of a bi-state quantizer. Compared in Figs. 6-2.1 and 6-2.2 is an ADM using a Kalman Filter with and without predictor employed. The tracking outputs Y_k of an ADM decoder with predictor always fluctuate around the original input signals X_k .

Fig. 6-2.3 is a plot of both X_k , Y_k versus time with no Kalman Filter employed. With the same sinusoidally biased signal input as before, the tracking output of the ADM decoder without a Kalman Filter

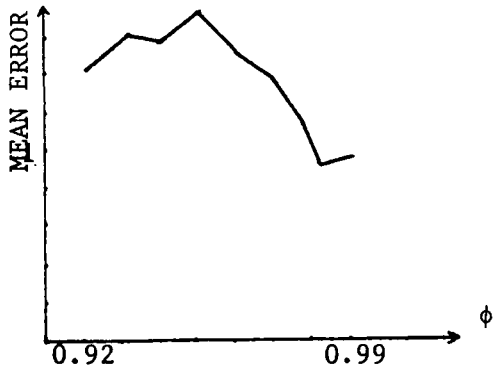
Table 1. Data of the Mean Errors (with IX=666699, IY=65549)

		$\phi=0.92$	$\phi=0.93$	$\phi=0.94$	$\phi=0.95$	$\phi=0.96$	$\phi=0.97$	$\phi=0.98$	$\phi=0.99$
Bi-state Quanti- zer	Type 1 *	1.397413	1.565342	1.543120	1.709801	1.403490	1.343197	0.9114966	0.979419
	Type 2 **	1.979756	1.926772	1.800747	2.210831	1.696623	1.496176	1.291538	1.147225
	Type 3 ***	2.093743	1.976157	1.842721	1.703469	1.576509	1.465842	1.468191	1.222938
Tri- state Quanti- zer	Type 1	1.153731	0.971534	0.958715	0.852457	0.727492	0.534385	0.581324	0.534170
	Type 2	1.675919	1.436068	1.345751	1.266820	1.309594	1.070161	0.998598	0.457840
	Type 3	2.044930	1.929339	1.625833	1.494823	1.405892	1.136147	0.919527	0.751769

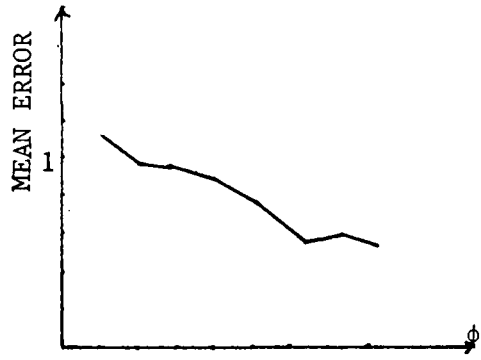
* Encoding System with Kalman Filter and Predictor.

** Encoding System with Kalman Filter, but without Predictor.

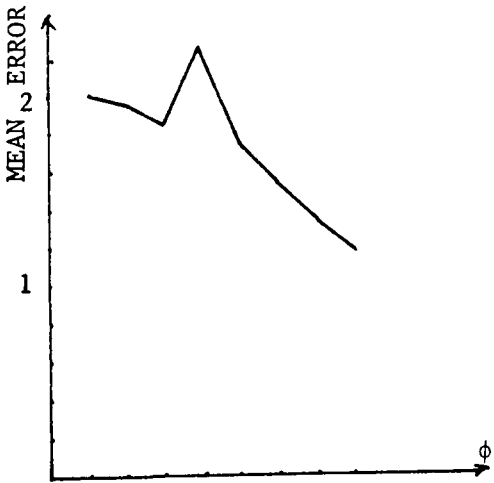
*** Encoding System Withour Kalman Filter.



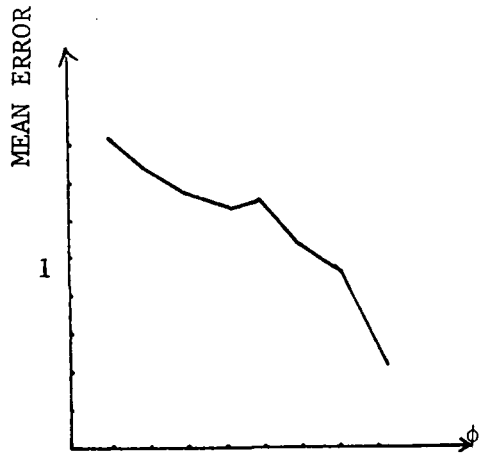
Type 1 (with Bi-state Quantizer).



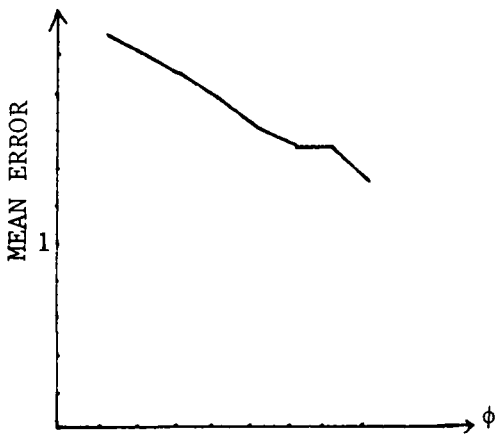
Type 1 (with Tri-state Quantizer).



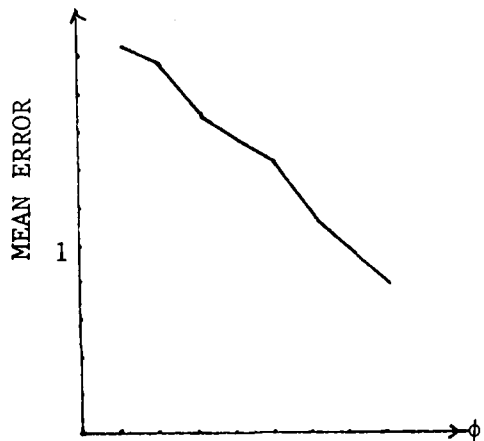
Type 2 (with Bi-state Quantizer)



Type 2 (with Tri-state Quantizer)



Type 3 (with Bi-state Quantizer)



Type 3 (with Tri-state Quantizer)

Figure 6-1.1.

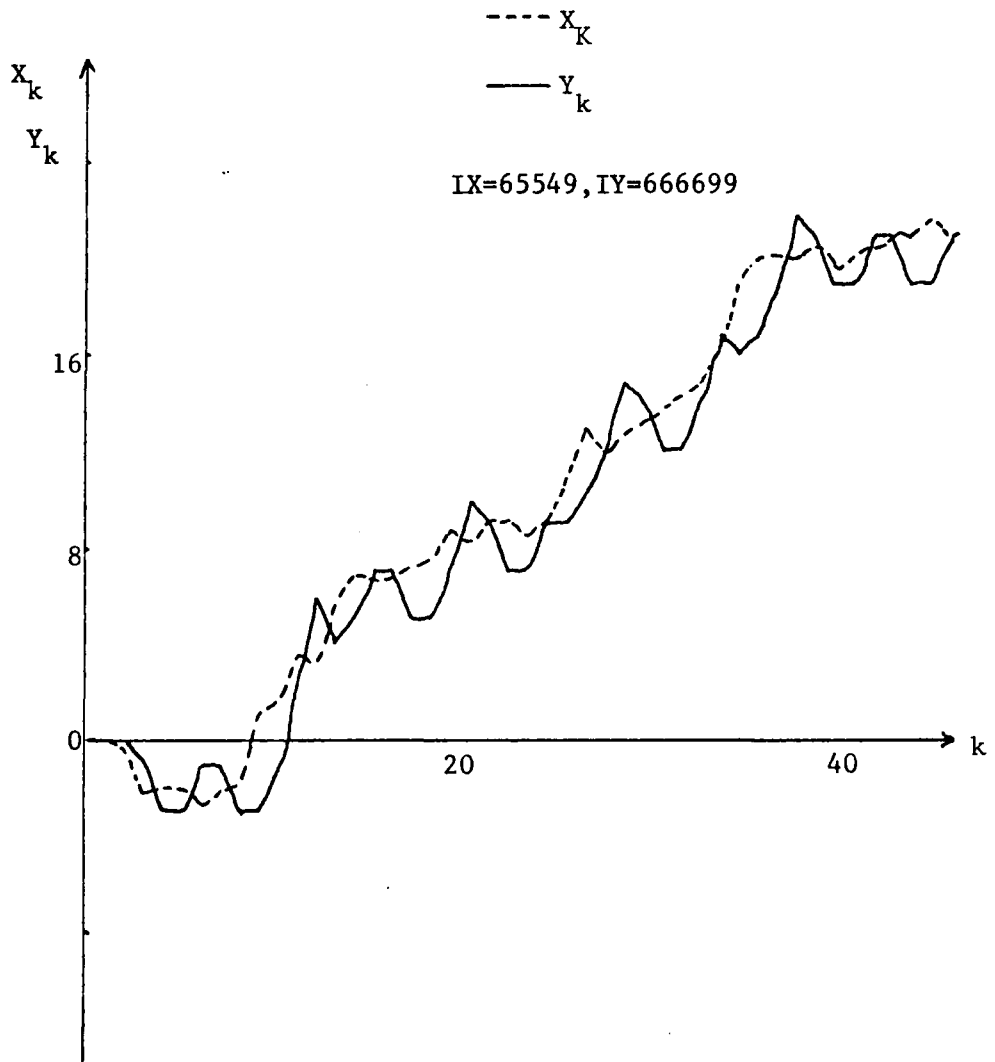


Figure 6-2.1. Type 1 Encoding with Bi-state Quantizer.

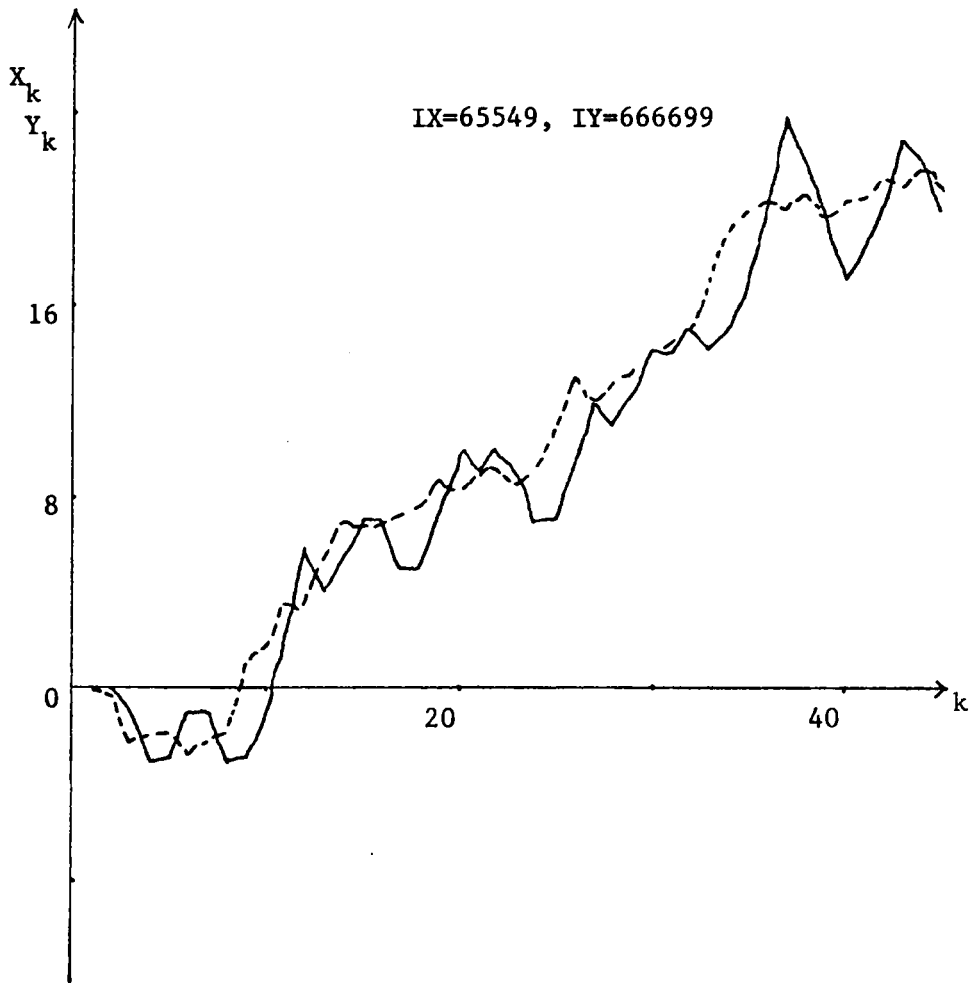


Figure 6-2.2. Type 2 Encoding with Bi-state Quantizer.

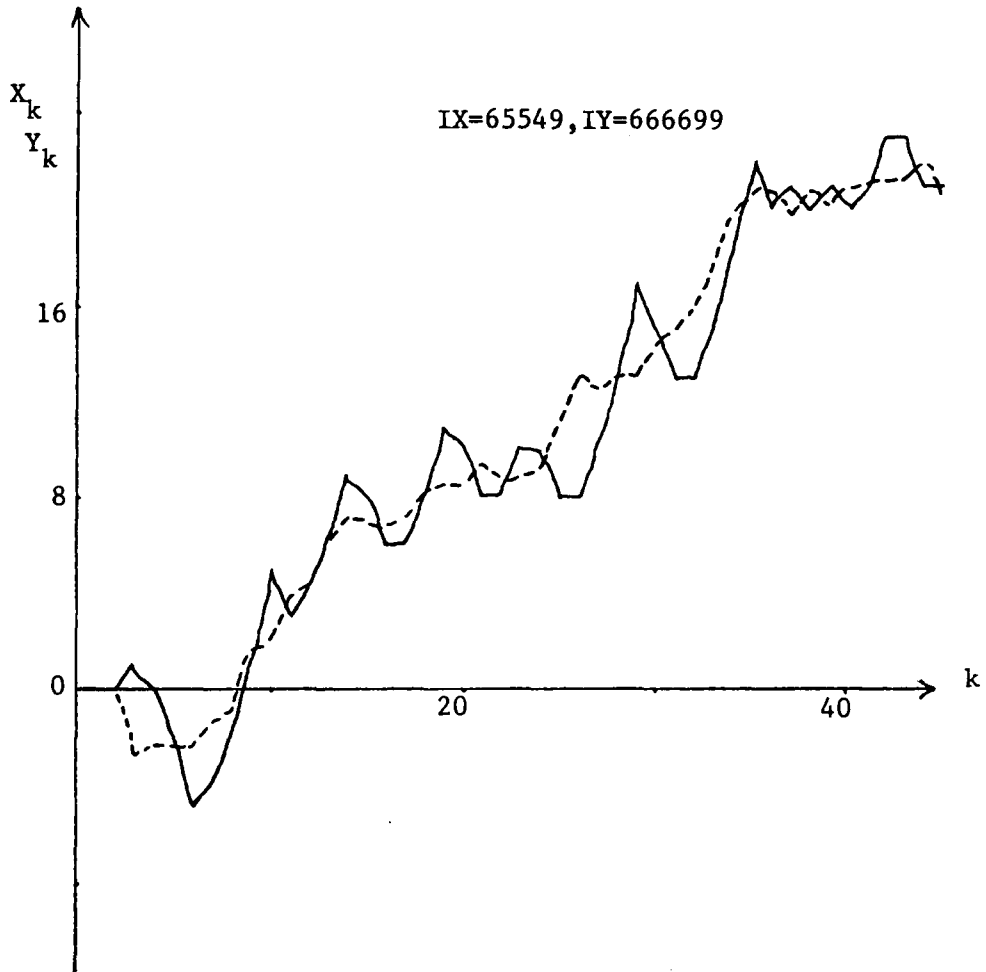


Figure 6-2.3. Type 3 Encoding with Bi-state Quantizer.

is shown to have a larger fluctuation which results in a larger error.

The operation of using the tri-state quantizer in place of the bi-state quantizer, the rest of the device remaining the same as that for Figs. 6-2.1, 6-2.2, 6-2.3, is shown in Figs. 6-2.4, 6-2.5, 6-2.6 respectively. The idle and overload noises are reduced which also results in a reduction in the oscillation amplitude of the tracking signals Y_k as compared with the X_k signals.

The ADM is an on-line tracking device, i.e. Y_k are calculated from the past data of X_k . In other words, Y_k are estimated from the past values X_1, X_2, \dots, X_{k-1} ; therefore, Y_k always emulate X_{k-1} . If we advance the Y_k signals one time step, or if we delay X_k by one time step, and then compare X_{k-1} and Y_k , the results from the same input data as in Figs. 6-2.1 to 6-2.6 are redrawn in Figs. 6-2.7 to 6-2.12 respectively. The tracking or estimated Y_k are closely coincident with the input signals X_k of the ADM as shown in Fig. 6-2.10 when the Kalman Filter and predictor are connected to the ADM and the tri-state quantizer is employed.

Figs. 6-2.13 to 6-2.18 show a change of the Gaussian noise input. This is done by changing the seeds in the generation of the artificial Gaussian noise generator of the computer; however, the mean value and the variance of the noise are kept the same. In correspondence with Figs. 6-2.7 to 6-2.12, the results are shown in Figs. 6-2.13 to 6-2.18 which are as satisfactory as the previous results, indicating an insensitivity to the specific noise waveform.

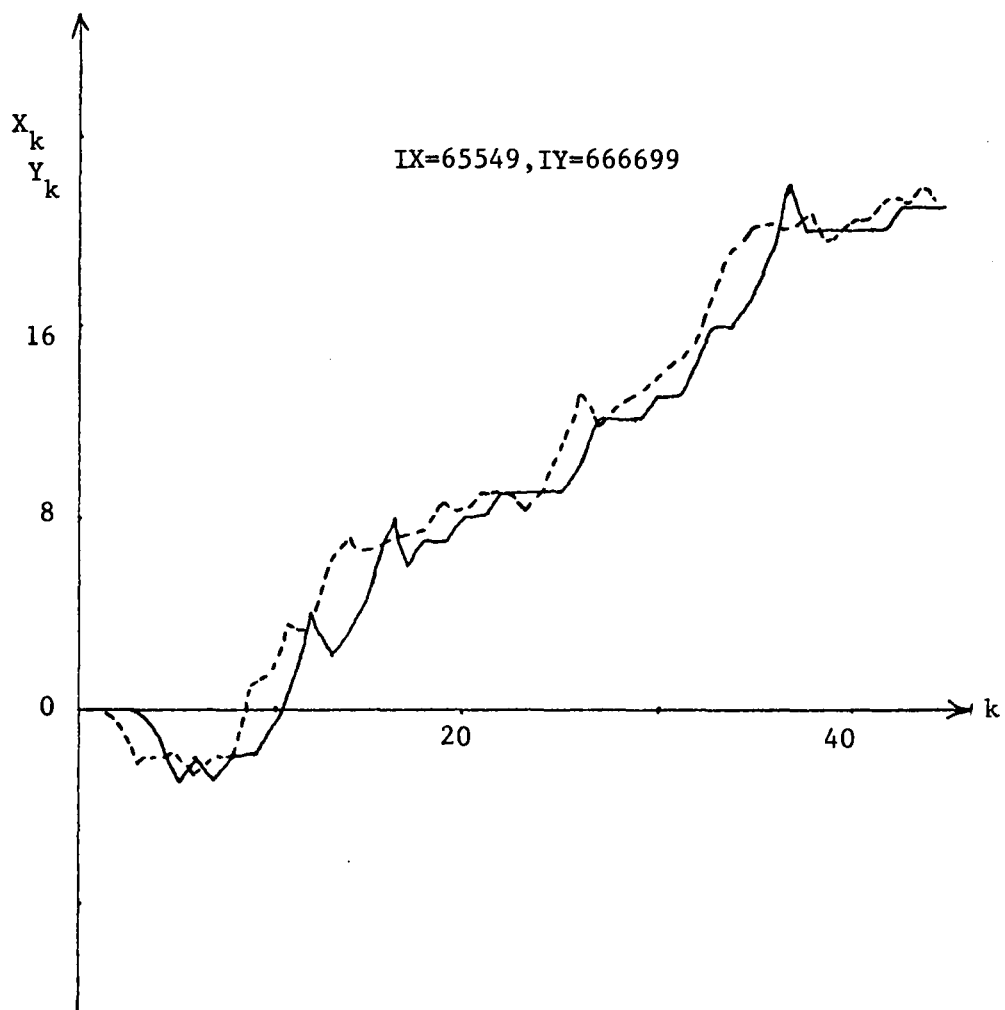


Figure 6-2.4. Type 1 Encoding with Tri-state Quantizer.

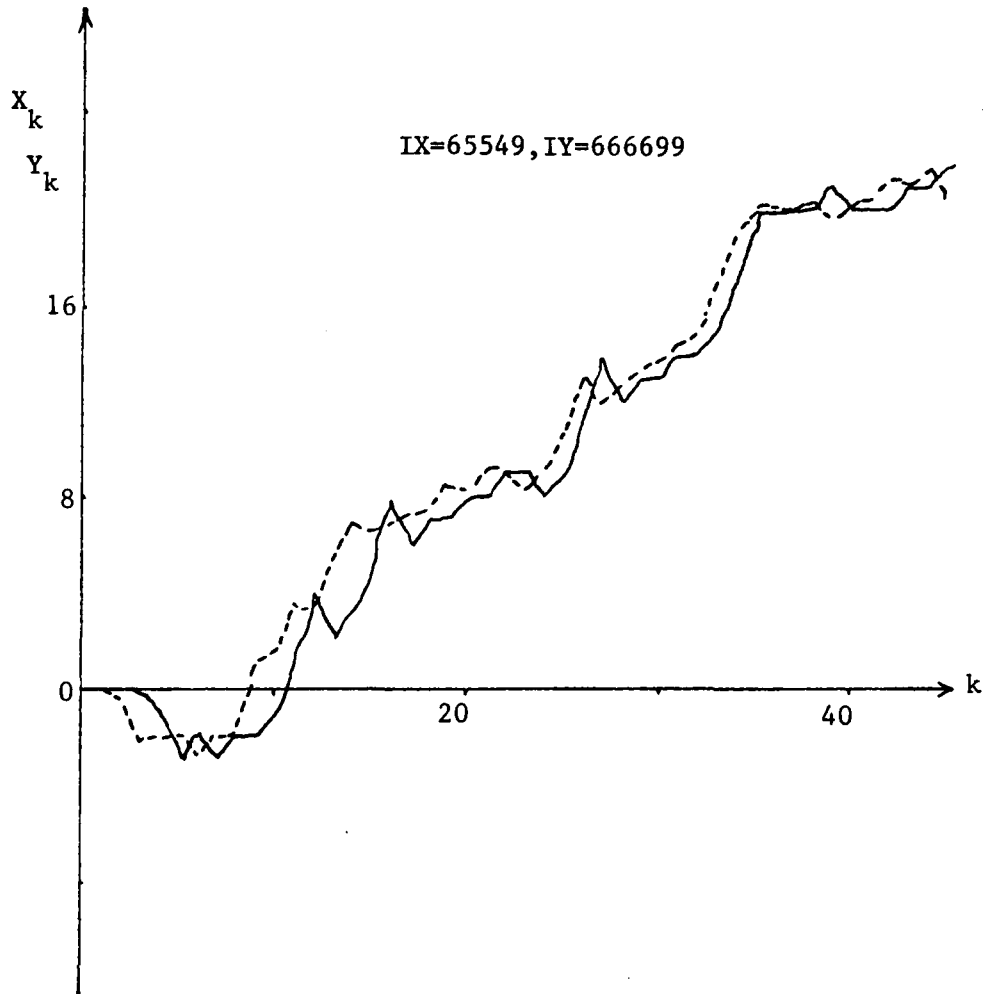


Figure 6-2.5. Type 2 Encoding with Tri-state Quantizer.

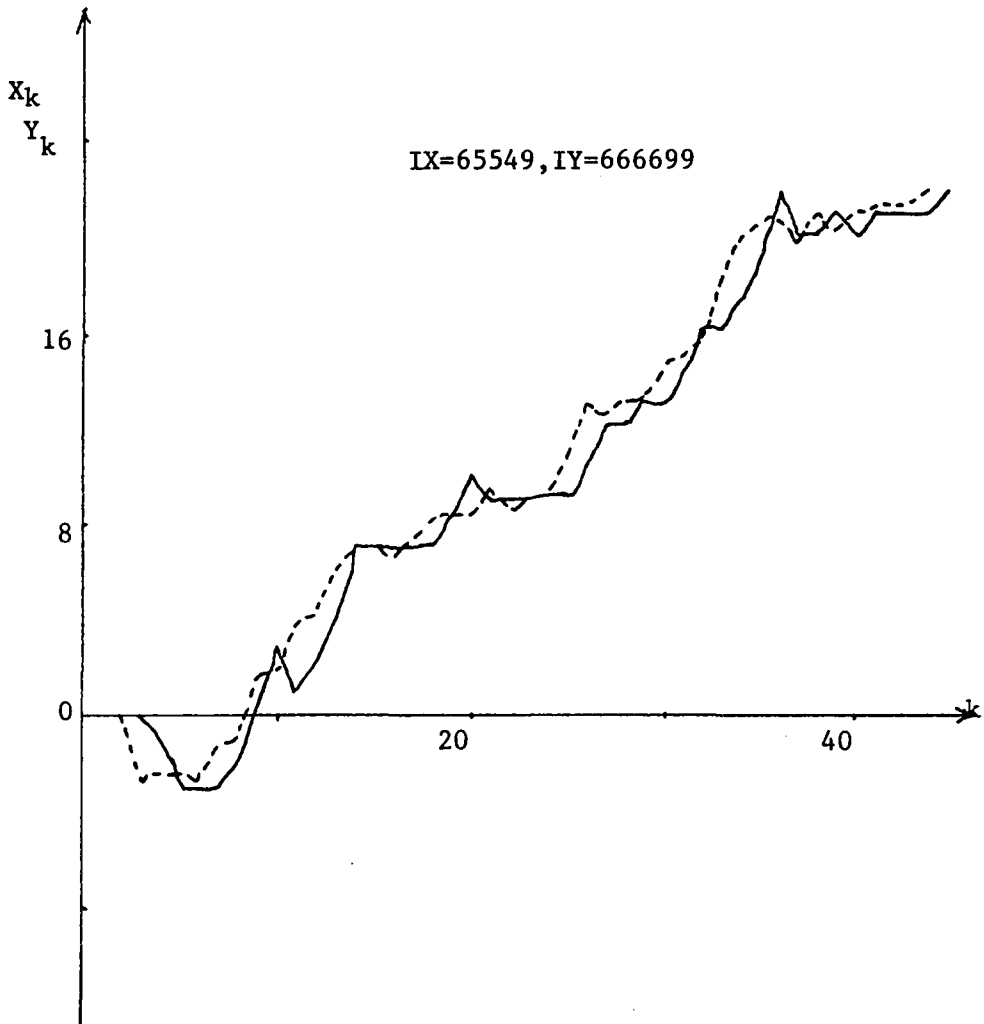


Figure 6-2.6. Type 3 Encoding with Tri-state Quantizer.

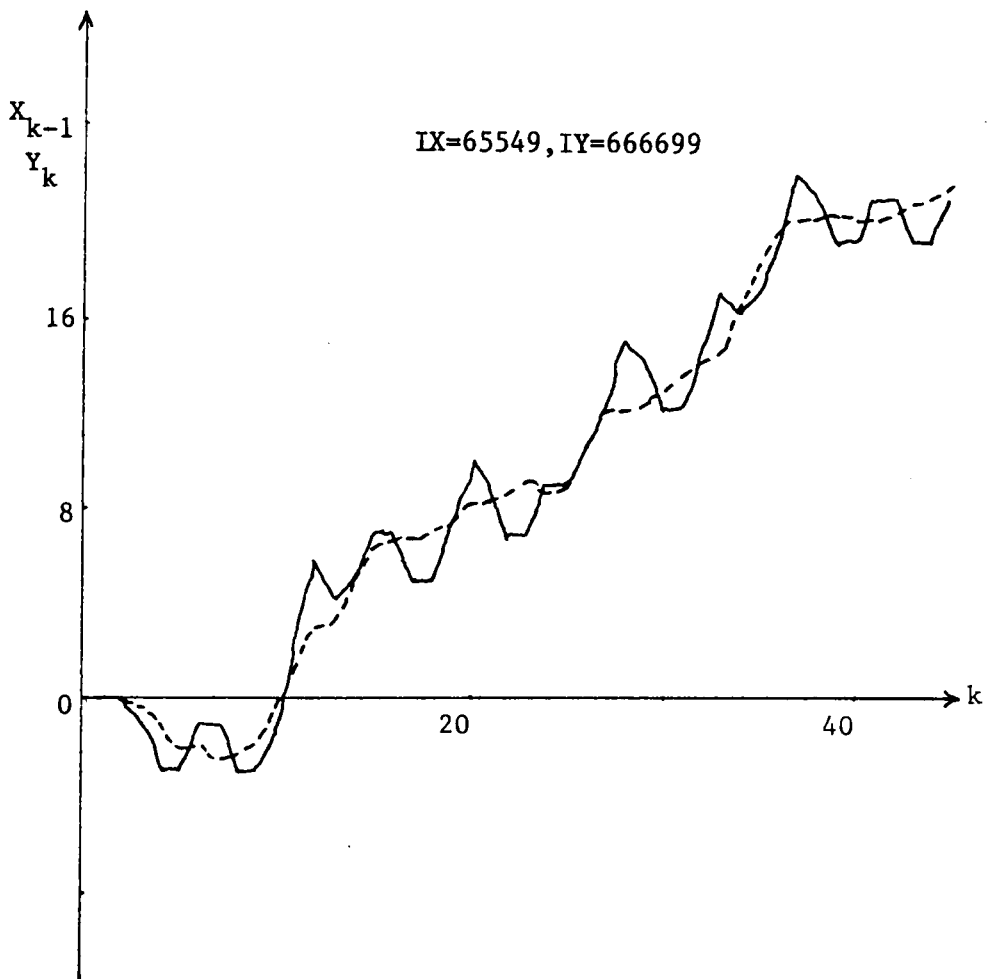


Figure 6-2.7. Type 1 Encoding with Bi-state Quantizer.

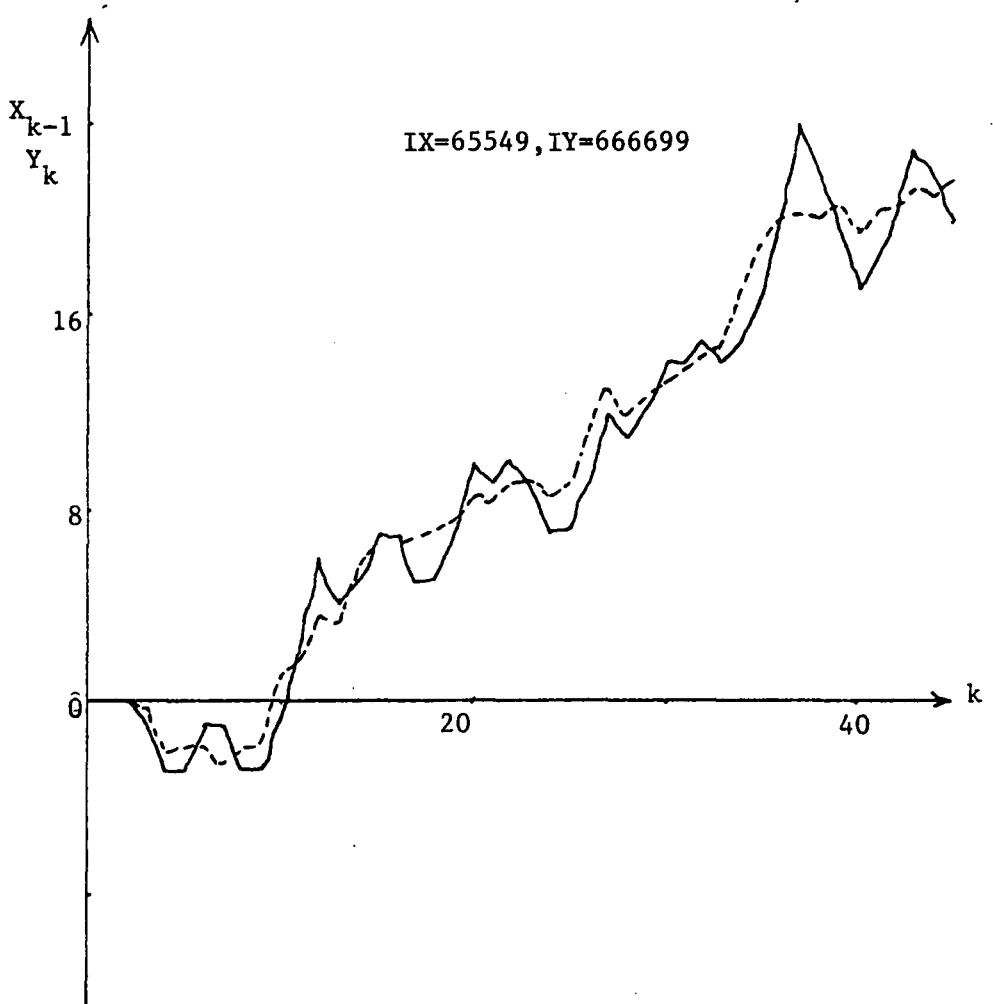


Figure 6-2.8. Type Encoding with Bi-state Quantizer.

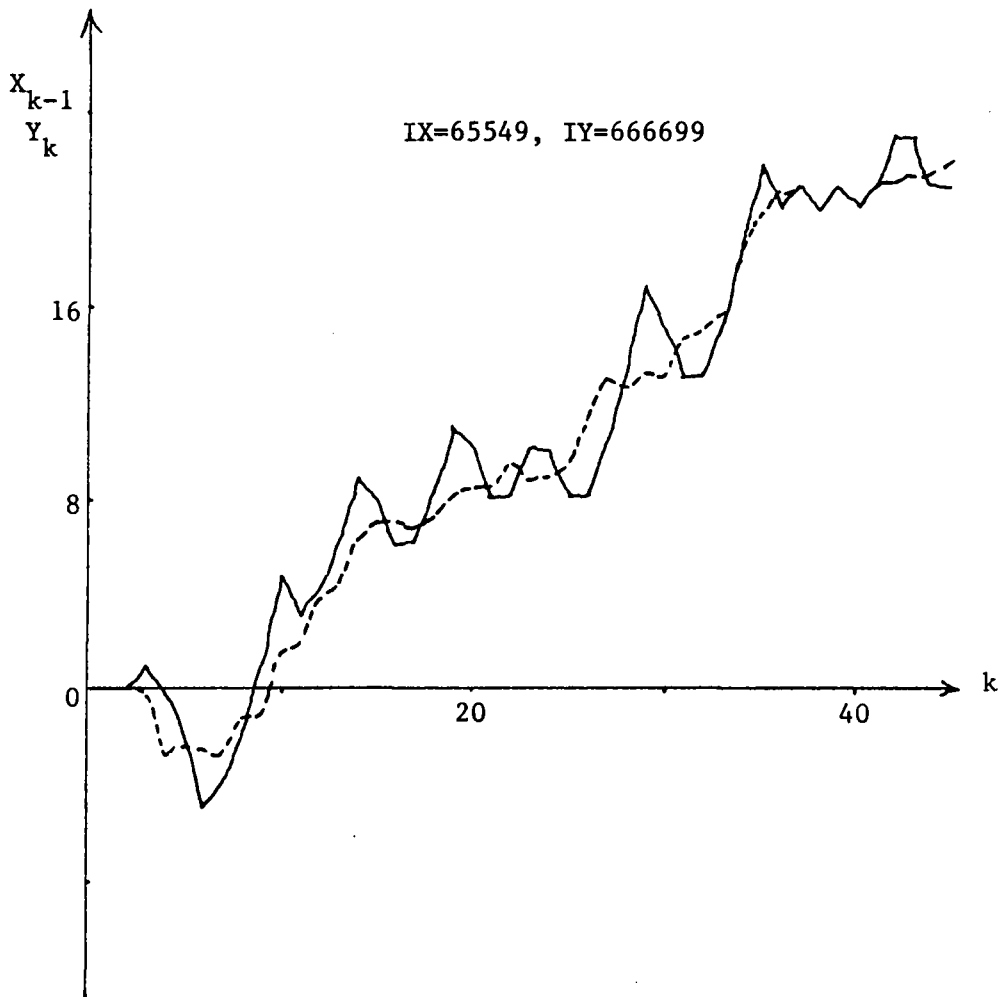


Figure 6-2.9. Type 3 Encoding with Bi-state Quantizer.

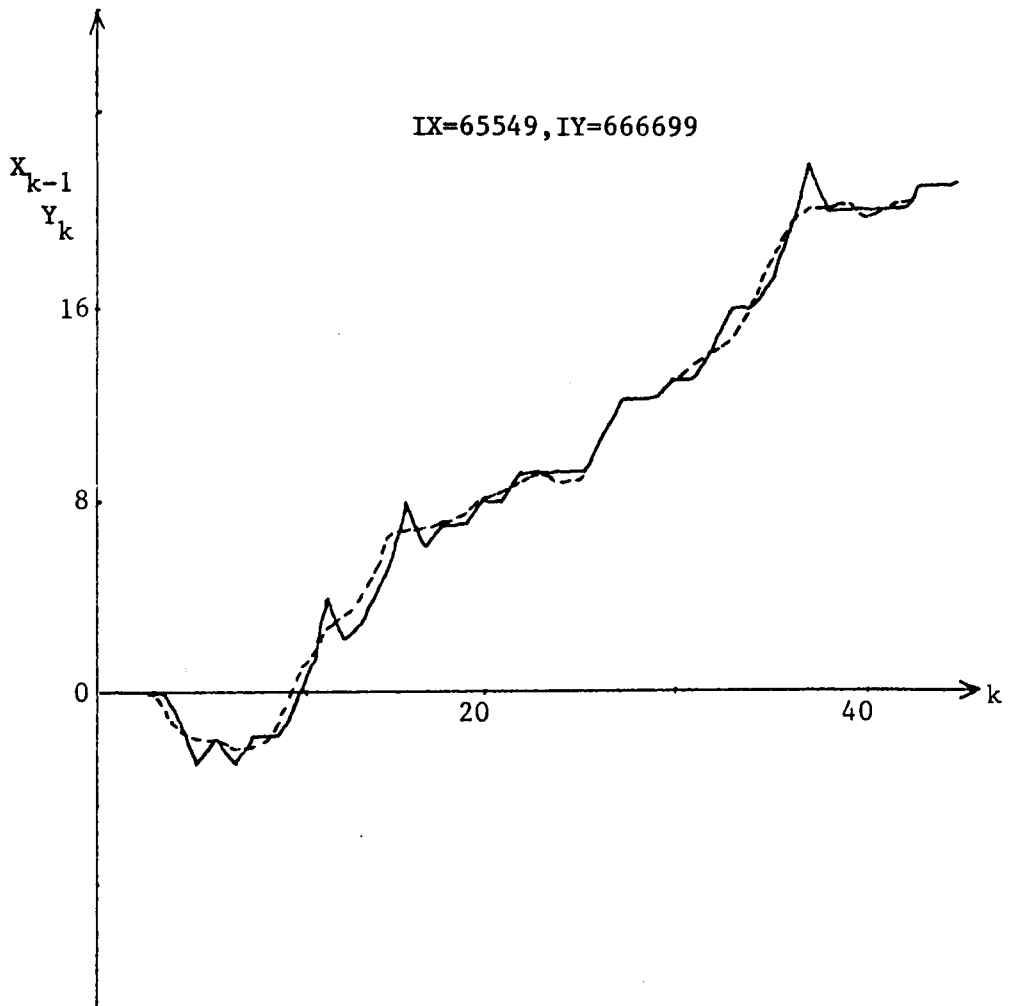


Figure 6-2.10. Type 1 Encoding with Tri-state Quantizer.

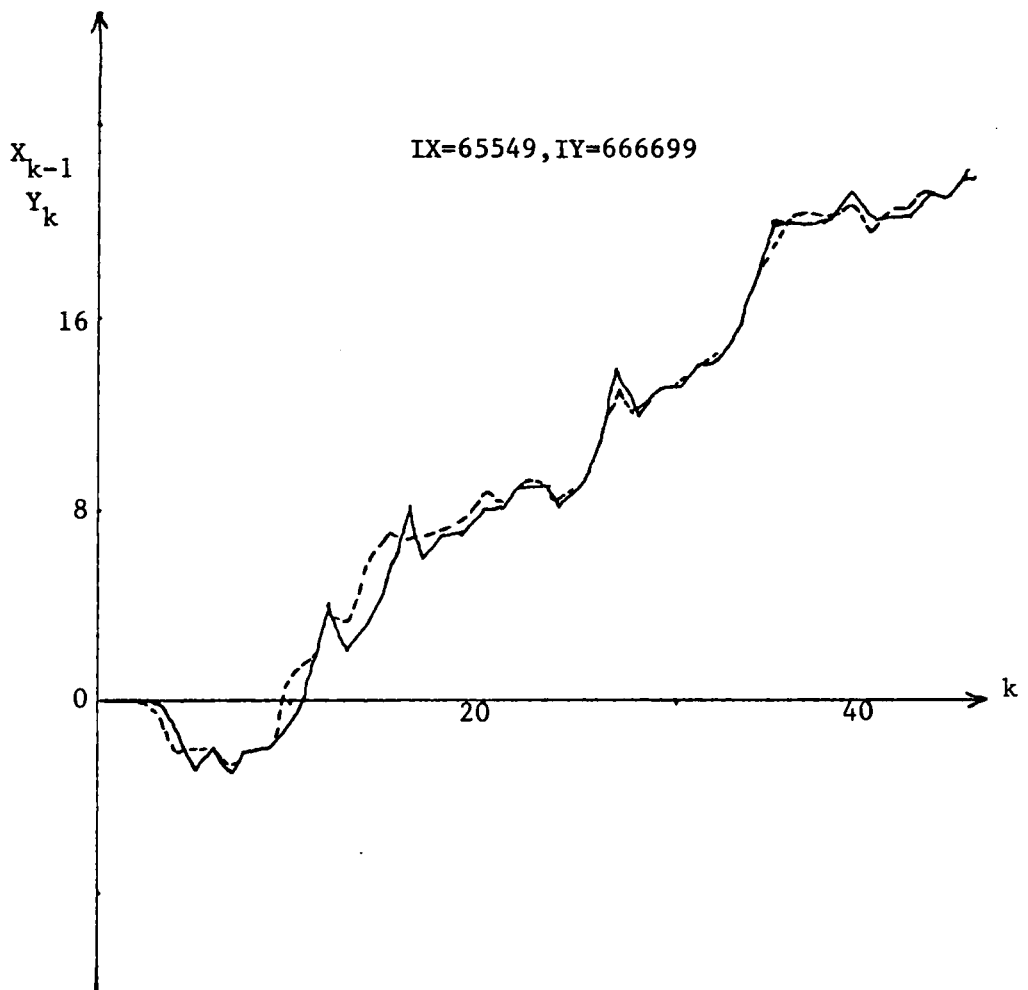


Figure 6-2.11. Type 2 Encoding with Tri-state Quantizer.

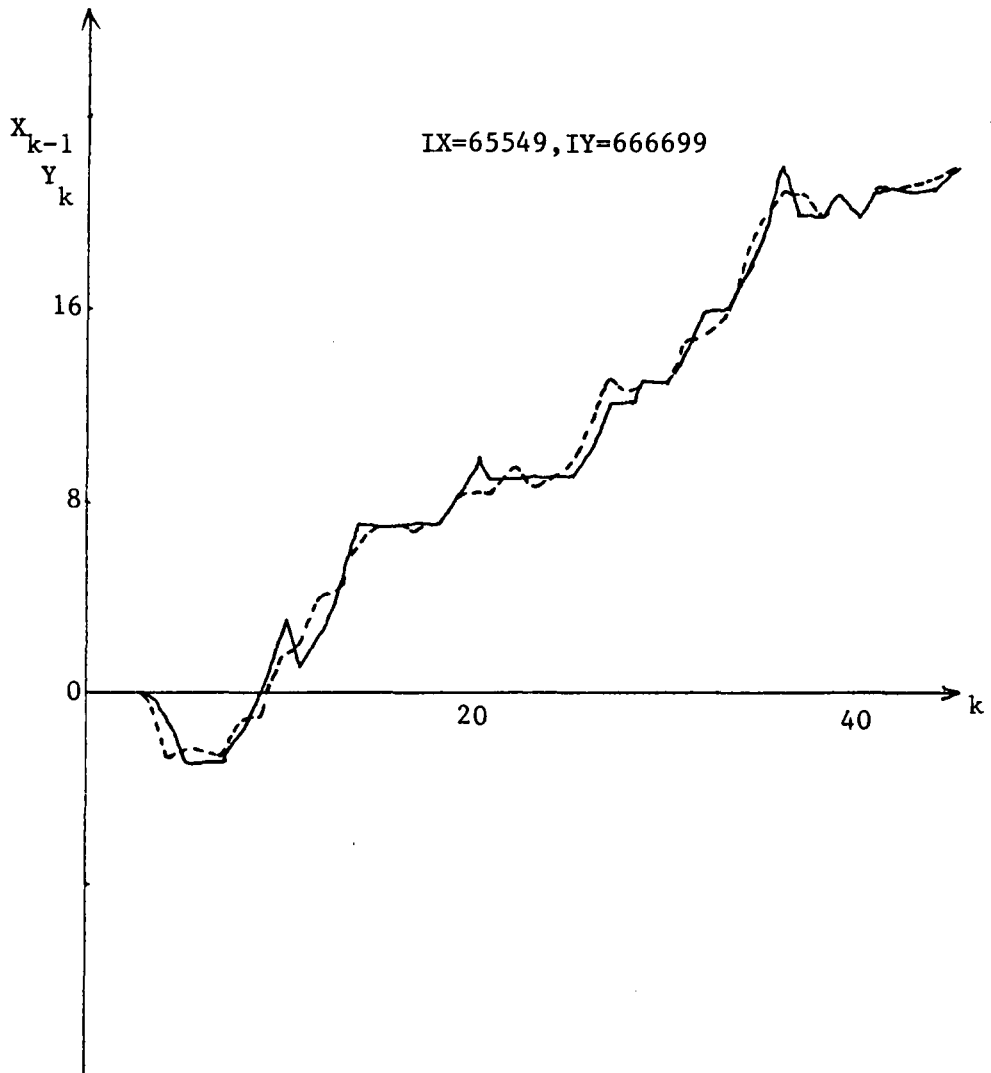


Figure 6-2.12. Type 3 Encoding with Tri-state Quantizer.

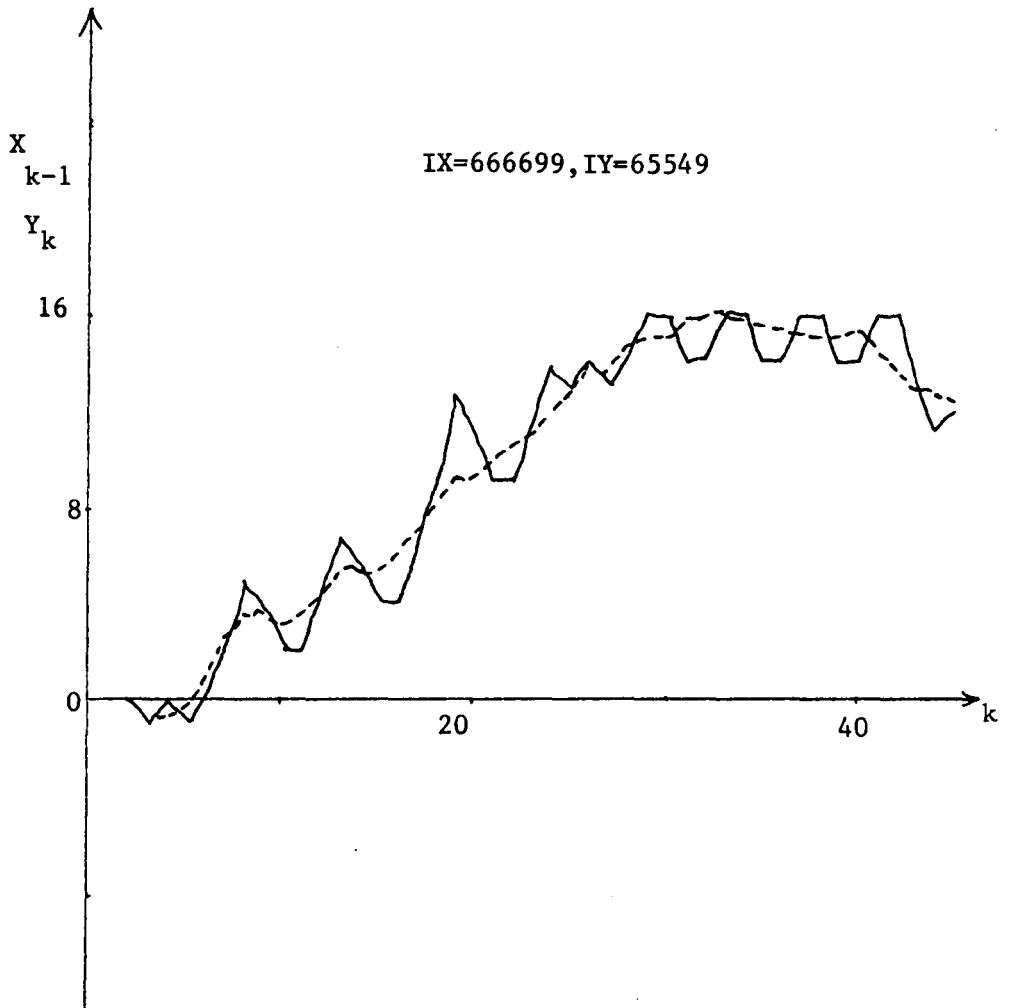


Figure 6-2.13. Type 1 Encoding with Bi-state Quantizer.

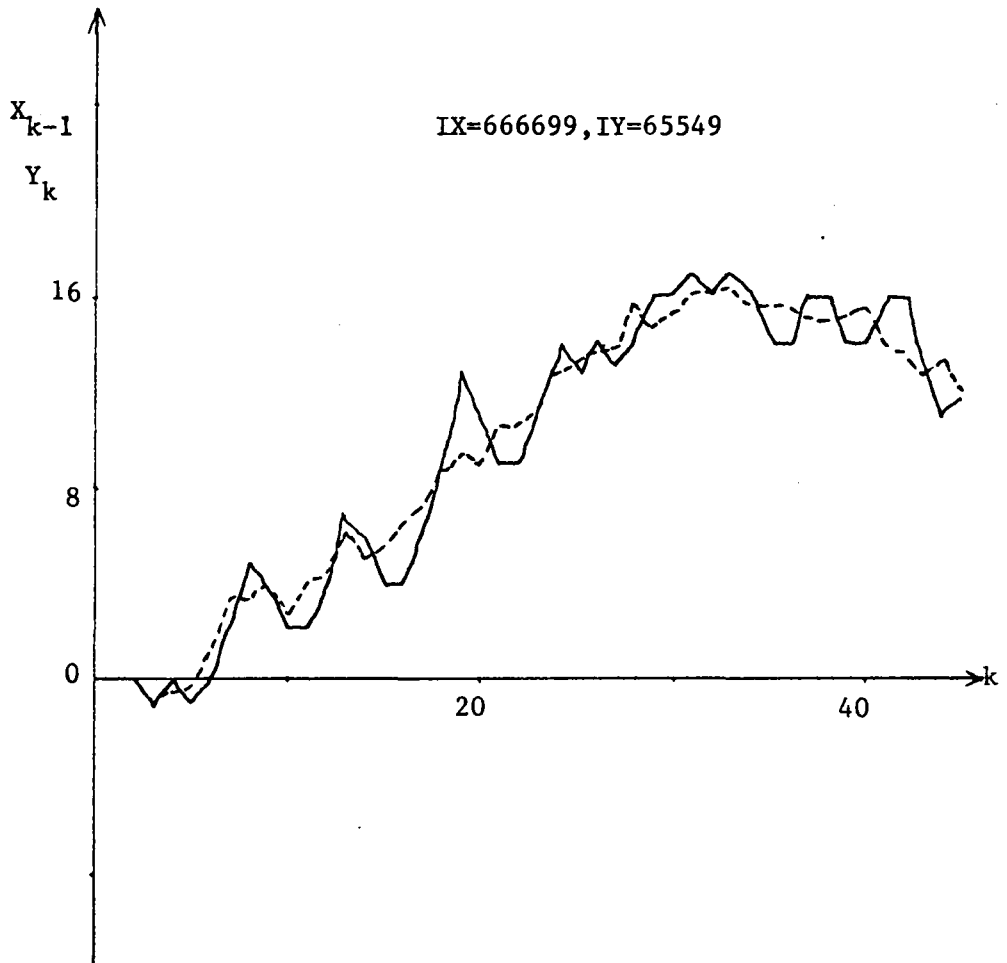


Figure 6-2.14. Type 2 Encoding with Bi-state Quantizer.

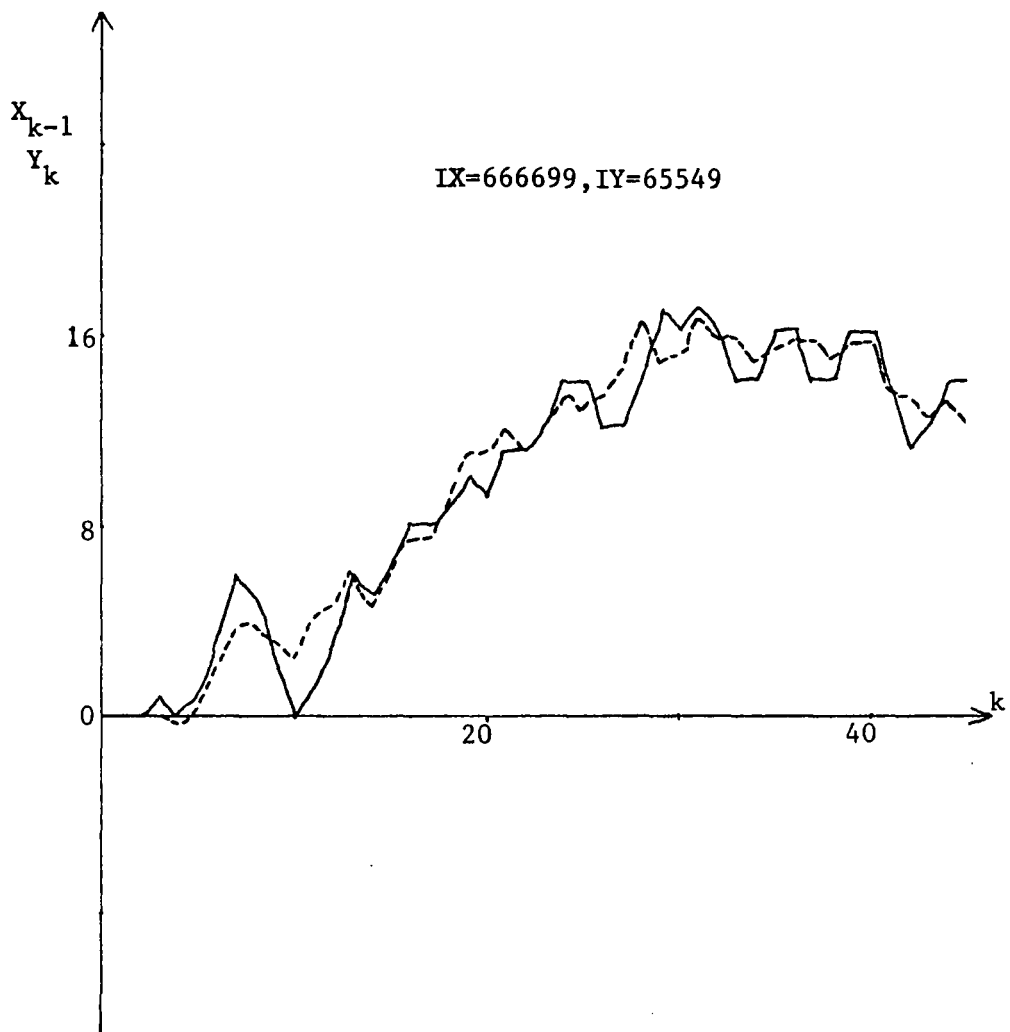


Figure 6-2.15. Type 3 Encoding with Bi-state Quantizer.

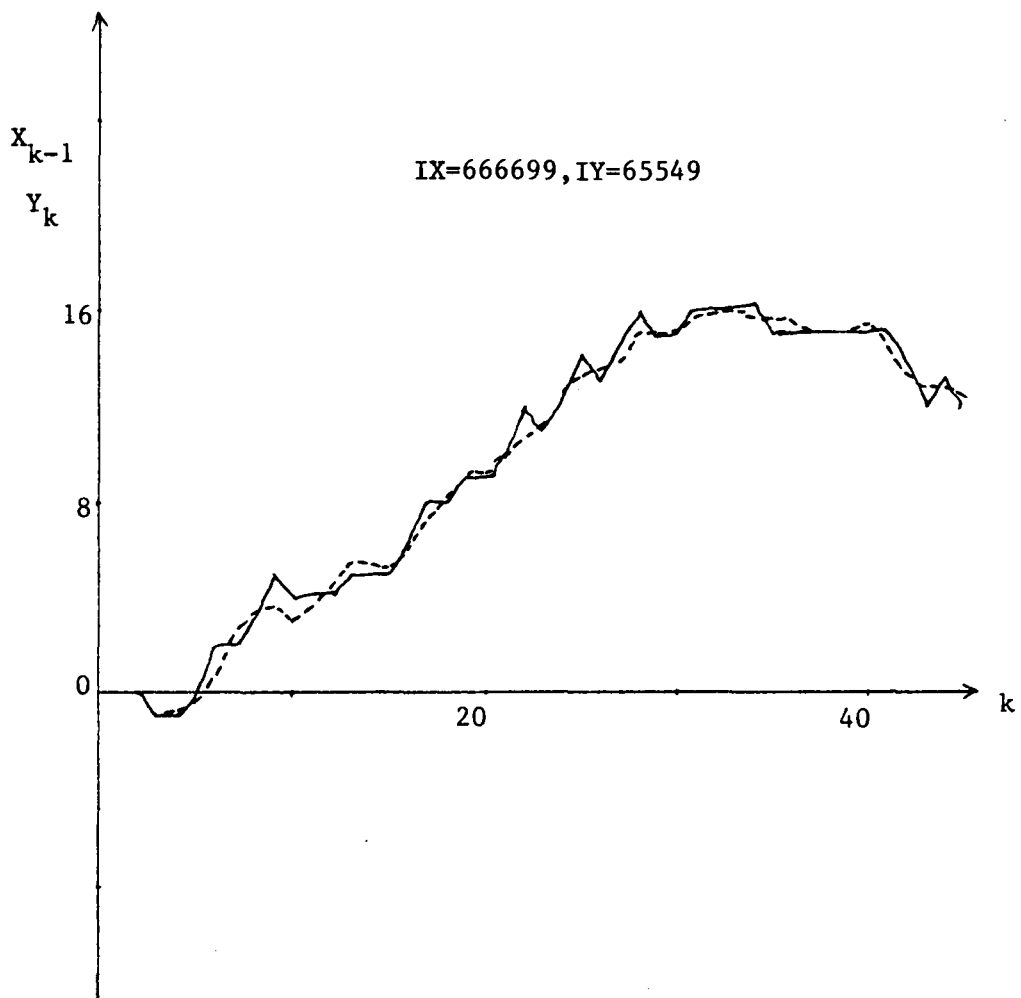


Figure 6-2.16. Type 1 Encoding with Tri-state Quantizer.

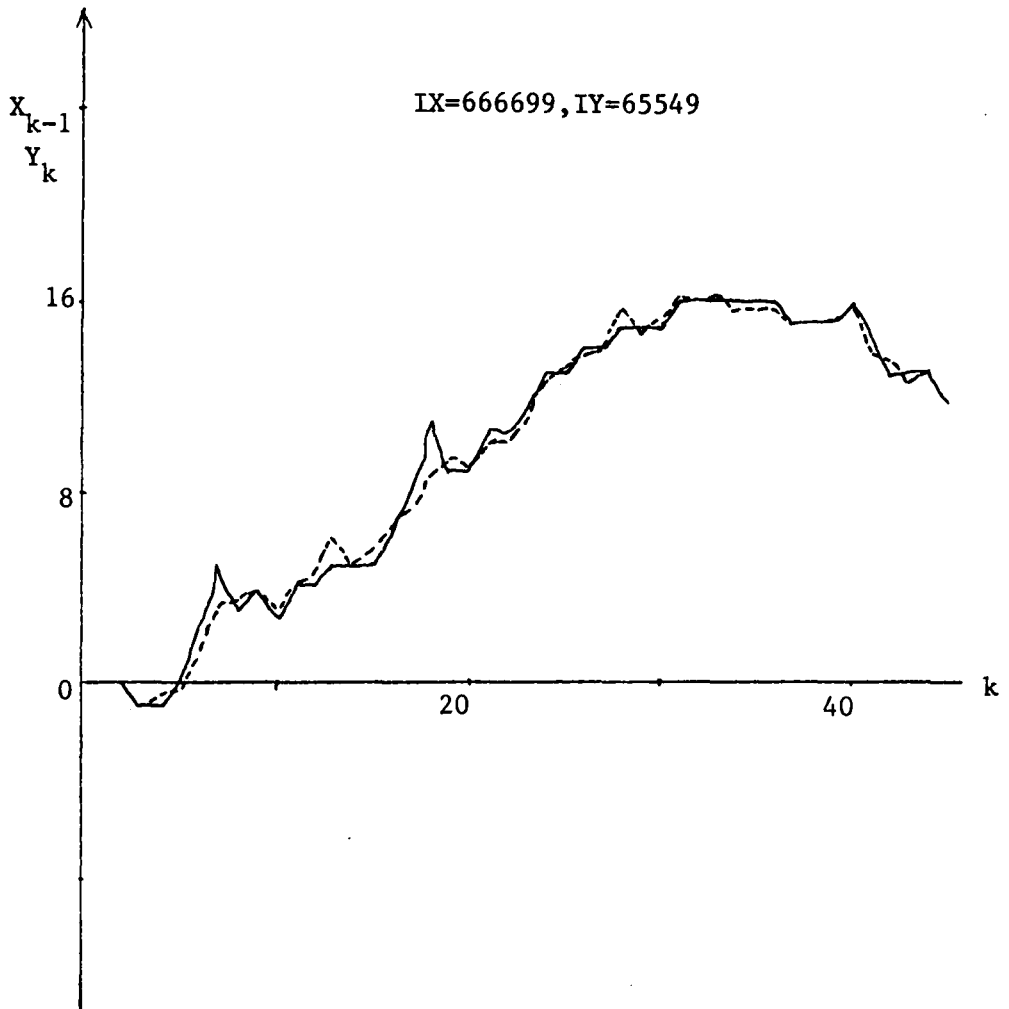


Figure 6-2.17. Type 2 Encoding with Tri-state Quantizer.

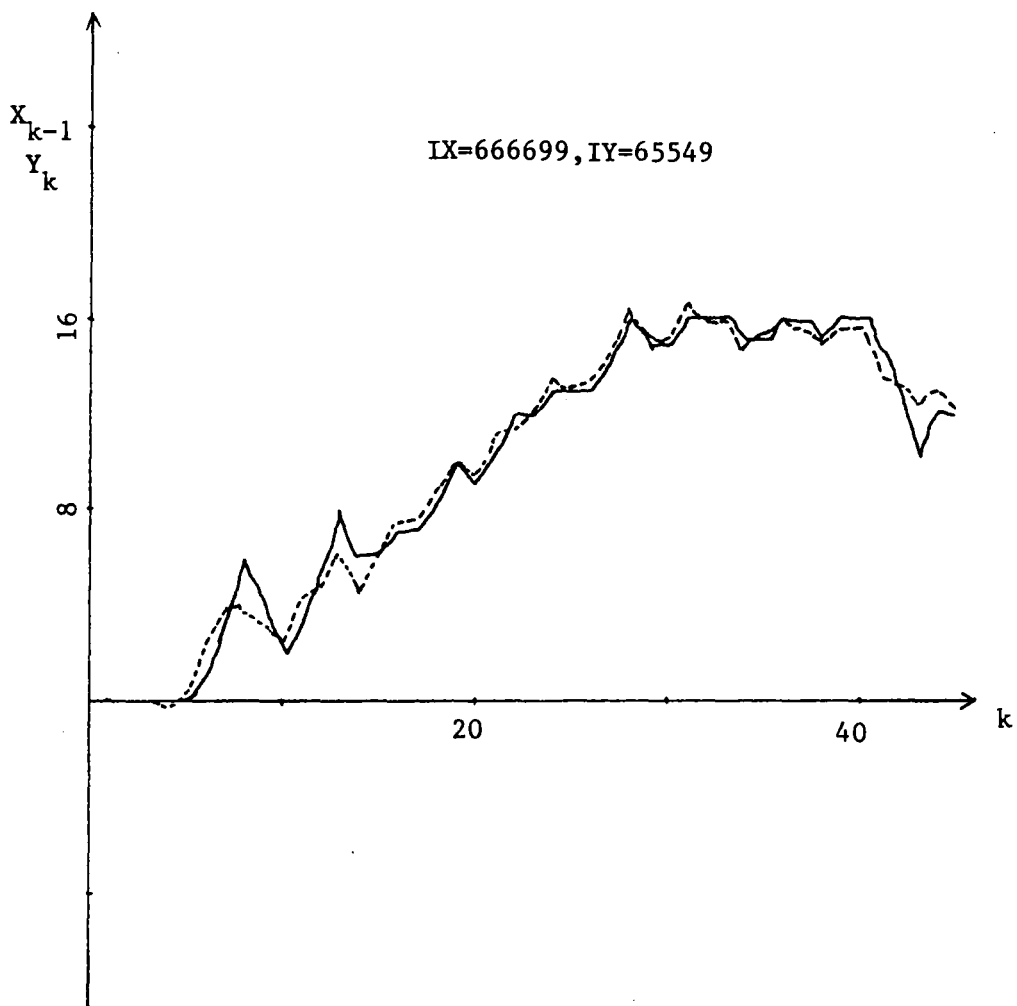


Figure 6-2.18. Type 3 Encoding with Tri-state Quantizer.

6-2. Conclusions

In this report, some innovations, e.g. the tri-state system, and detailed studies have been made on Adaptive Delta Modulators for the case of highly correlated messages. For such signals, the ADM provides reproducible modulated signals with a minimum of equipment. In addition, a number of variations were studied, including Kalman prefiltering and one-step prediction, which allow further error reduction beyond the basic ADM system.

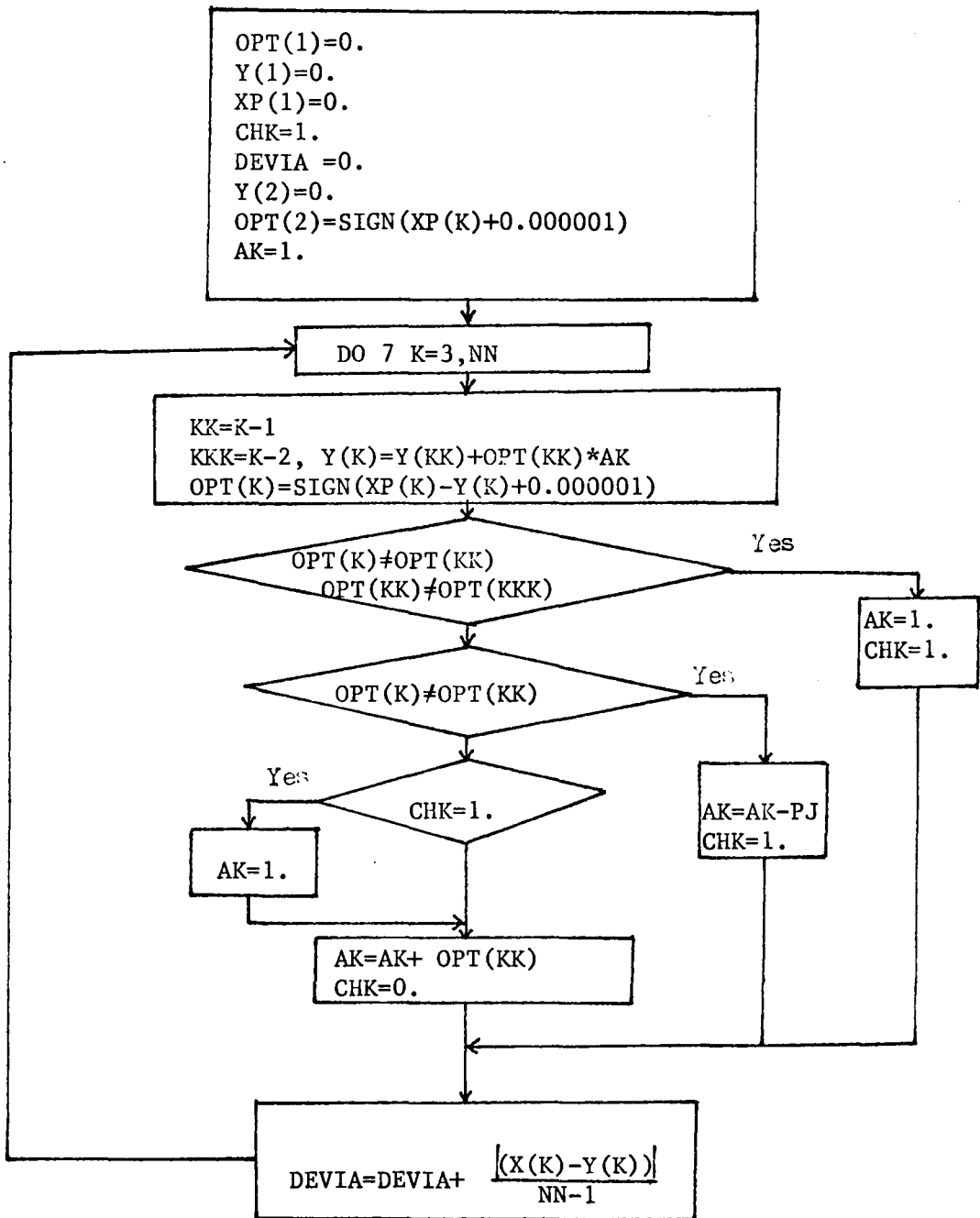
6-3. Recommendations

In the above discussion, the input signal used was a sinusoidally biased signal. Although not a completely general test function, it was useful to represent a rapidly sampled voice signal. A wider class of signals is, however, of interest in the general digital communication problem, for instance abruptly changing "control" signals. In addition, with low statistical correlation-representing e.g. a low sampling rate for an input analog signal.

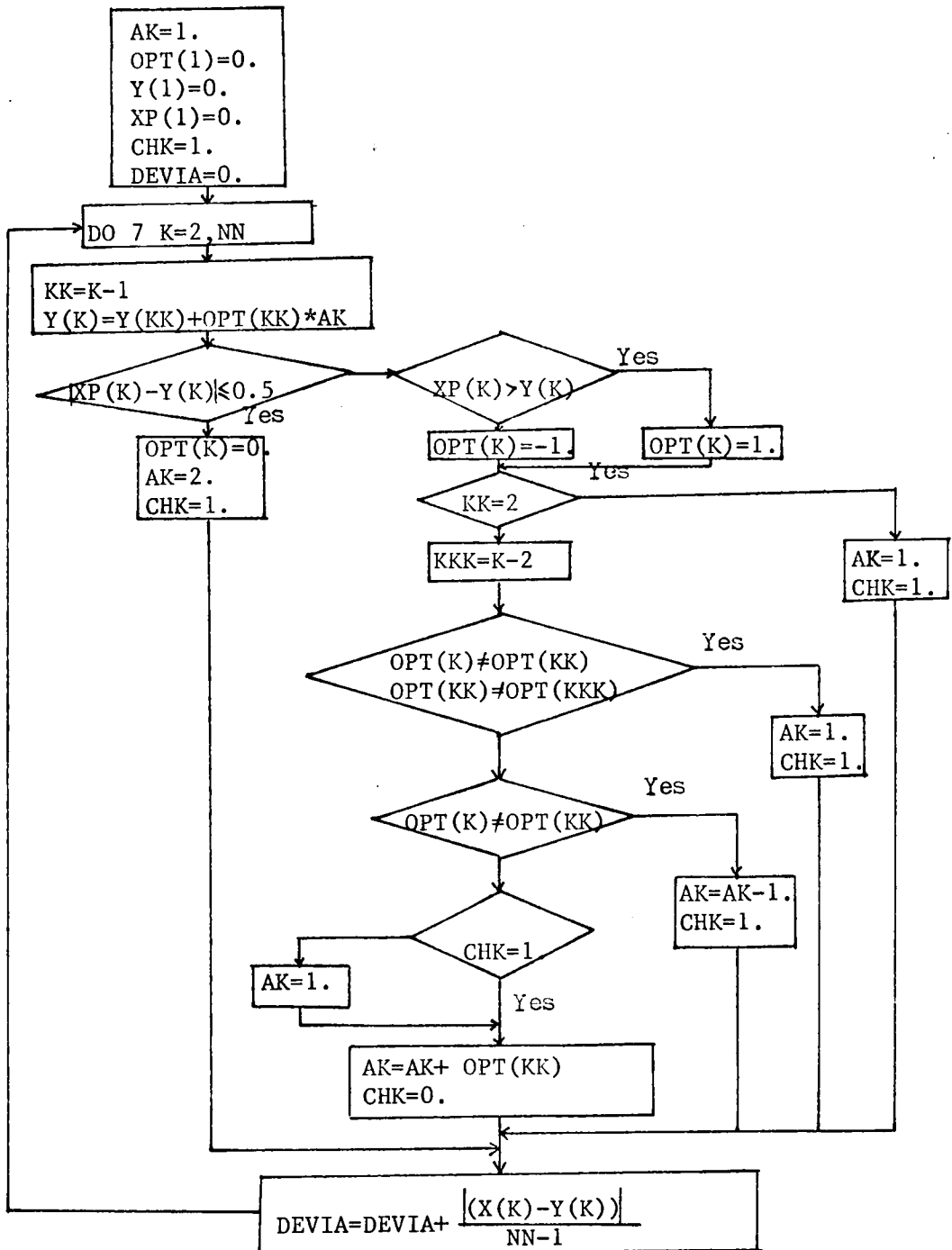
BIBLIOGRAPHY

1. Taub and Schilling, Principles of Communication Systems (New York: McGraw-Hill, Inc. 1971).
2. J.W. Bayless, S.J. Campanella, A.J. Goldberg, Voice Signals bit by bit, IEEE spectrum, pp 28-31, Oct. 1973.
3. David J. Goodman, A Digital Approach to Adaptive Delta Modulation The Bell System Technical Journal, April 1971.
4. A. Papoulis, Probability, Random Variables and Stochastic Processes (New York, McGraw-Hill, Inc. 1965).
5. H.F. VanLandingham, "Class Notes for EE 5401 (Discrete Time Systems), EE 5402 (Stochastic Control), EE 6400 (Stochastic Systems). Department of Electrical Engineering, Virginia Polytechnic Institute and State University, Blacksburg, Va.
6. J.S. Meditch, Stochastic Optimal Linear Estimation and Control (McGraw-Hill Book Company, 1969).
7. Arther Gelb, Applied Optimal Estimation (The M.I.T. Press, 1974).
8. M.R. Arron, Response of Delta Modulation to Gaussian Signals The Bell System Technical Journal, May-June 1969.

APPENDIX
COMPUTER PROGRAM LISTING



Flow Chart of a Bi-state ADM



Flow Chart of A Tri-state ADM

```

REAL N(45), NI(3,3), KG(3,1), KGZZ1I(3,1),KGGH(3,3)
DIMENSION V(45), O(3,3), E(3,1),U(3,1),ENI(3,1),OKVENI(3,1),XHV(3
1,1),H(1,3),ZZ1I(3,3),OXHV(3,1),OXHVU(3,1),HP(1,3),HT(3,1),HPHT(1,
11),R2I(3,3),OP(3,3),OPR2I(3,3),CI(3,3),CKGH(3,3),OCKGH(3,3),OT(3,3
1),POT(3,3),RR(3,3),ET(1,3),EET(3,3),EQET(3,3),B(1,3),XH(1,1),X(45)
1,XP(45),Y(45),Q(45),OPT(45),XV(3,1),Z(45),HXHV(1,1),P(3,
13),OXV(3,1),QQ(3,3),XNKF(45),XXNKF(45),XXXNKF(45),XS(45),
1YS(45),XNKFS(45),XQ(45)
O(1,1)=0.994
O(2,1)=O(1,1)-1.
O(3,1)=O(2,1)
E(1,1)=10.*((1.+O(1,1))*(1.-O(1,1)))***0.5
NN=45
H(1,1)=1.
H(1,2)=0.
H(1,3)=0.
XHV(1,1)=0.
XHV(2,1)=0.
XHV(3,1)=0.
XV(1,1)=0.
XV(2,1)=0.
XV(3,1)=0.
B(1,1)=1.
B(1,2)=1.
B(1,3)=0.5
CALL SUBI(1.,P)
O(1,2)=0.
O(1,3)=0.
O(2,2)=0.
O(2,3)=0.
O(3,2)=-1.
O(3,3)=0.
E(2,1)=E(1,1)
E(3,1)=E(1,1)

```

```

DO 99 I=1,3
HT(I,1)=H(1,I)
ET(1,I)=E(I,1)
DO 99 J=1,3
99 OT(I,J)=O(J,I)
IX=65549
IY=666699
DO 1 K=2,NN
CALL GAUSS(IX,1.0,0.,N(K))
1 CALL GAUSS(IY,0.5,0.,V(K))
DO 2 K=2,NN
XNKF(K)=XV(1,1)
XXNKF(K)=XV(2,1)
XXXNKF(K)=XV(3,1)
Z(K)=XV(1,1)+V(K)
CALL GMPRD (0,XV,OXV,3,3,1,9,3,3)
CALL SUBI (N(K),NI)
CALL GMPRD (NI,E,ENI,3,3,1,9,3,3)
U(1,1)=20.*SIN( /80.*(K-1))-O(1,1)*SIN( /80.*(K-2
1))
U(2,1)=U(1,1)
U(3,1)=U(1,1)
CALL GMADD (OXV, ENI,OXVENI,3,1,3)
2 CALL GMADD (OXVENI,U,XV, 3,1,3)
DO 3 K=2,NN
CALL GMPRD (H,P,HP,1,3,3,3,9,3)
CALL GMPRD (HP,HT,HPHT,1,3,1,3,3,1)
R=0.5
R2=1./(HPHT(1,1)+R)
CALL GMPRD (O,P,OP,3,3,3,9,9,9)
CALL GMPRD (OP,R2I,OPR2I,3,3,3,9,9,9)
CALL GMPRD (OPR2I,HT, KG, 3,3,1,9,3,3)
CALL GMPRD (KG,H,KGH, 3,1,3,3,3,9)

```

```

CALL SUBI(-1., CI)
CALL GMPRD (CI, KGH, CKGH, 3, 3, 3, 9, 9, 9)
CALL GMADD (O, CKGH, OCKGH, 3, 3, 9)
CALL GMPRD (P, OT, POT, 3, 3, 3, 9, 9, 9)
CALL GMPRD (OCKGH, POT, RR, 3, 3, 3, 9, 9, 9)
CALL GMPRD (E, ET, EET, 3, 1, 3, 3, 3, 9)
CALL SUBI (1., QQ)
CALL GMPRD (QQ, EET, EQET, 3, 3, 3, 9, 9, 9)
CALL GMADD(RR, EQET, P, 3, 3, 9)
CALL GMPRD (H, XHV, HXHV, 1, 3, 1, 3, 3, 1)
Z1=HXHV(1, 1)
ZZ1=Z(K)-Z1
CALL SUBI (ZZ1, ZZ1I)
CALL GMPRD (ZZ1I, KG, KGZZ1I, 3, 3, 1, 9, 3, 3)
CALL GMPRD (O, XHV, OXHV, 3, 3, 1, 9, 3, 3)
CALL GMADD (OXHV, U, OXHVU, 3, 1, 3)
CALL GMADD (OXHVU, KGZZ1I, XHV, 3, 1, 3)
CALL GMPRD (B, XHV, XH, 1, 3, 1, 3, 3, 1)
XP(K)=XH(1, 1)
3 X(K)=XHV(1, 1)
Q(1)=0.1
DO 8 K=2, NN
Q(K)=K/10.
8 XQ(K)=XP(K)
S=-1.
102 OPT(K)=0.
Y(1)=0.
XQ(1)=0.
CHK=1.
DEVIA=0.
Y(2)=0.
OPT(2)=SIGN(1., XQ(2))+0.000001)
AK=1.

```

```

DO 7 K=3,NN
KK=K-1
KKK=K-2
Y(K)=Y(kk)+OPT(KK)*AK
OPT(K)=SIGN(1.,XQ(K)-Y(K)+0.000001)
IF (OPT(K).NE.OPT(KK).AND.OPT(KK).NE.OPT(KKK))) GO TO 11
IF (OPT(K).NE.OPT(KK)) GO TO 12
IF (CHK.EQ.1.) GO TO 14
15 AK=AK+ABS(OPT(KK))
CHK=0.
GO TO 7
11 AK=1.
CHK=1.
GO TO 7
12 AK=ABS(AK-2)
CHK=1.
GO TO 7
14 AK=1.
GO TO 15
7 DEVIA=DEVIA+ABS(XQ(KK)-Y(K))/(NN-1)
PRINT,DEVIA
PRINT 16, (XQ(K),K=1,45)
PRINT 16, (Y(K), K=1,45)
16 FORMAT (14(F 8.2,1X))
XS(1)=0.
YS(1)=0.
DO 4 K=2,NN
KK=K-1
XS(K)=XQ(KK)/8.
4 YS(K)=Y(K)/8.
IF (S.EQ. -1.) CALL PLOT (0.6,5.5,-3)
CALL AXIS (0.0,0.0,'K',-1,5.0,0.0,1.0,10.0)
CALL AXIS (0.0,-5.0,'X,Y',3,10.0,90.0,-40.0,8.0)
CALL PLOT (0.0,0.0,3)

```



```
CALL LINE (Q,XS,45,-1)
CALL PLOT (0.0,0.0,3)
CALL LINE (Q,YS,45,-1)
CALL PLOT (0.0,0.0,3)
CALL PLOT (7.0,0.0,-3)
IF (S) 106,107,100
106 DO 101 K=2,NN
101 XQ(K)=X(K)
    S=0.
    GO TO 102
107 DO 104 K=2,NN
104 XQ(K)=XNKF(K)
    S=+1.
    GO TO 102
100 S=-1.
202 AK=1.
    OPT(1)=0.
    Y(1)=0.
    XP(1)=0.
    CHK=1.
    DEVIA=0.
    DO 17 K=2,NN
        KK=K-1
        Y(K)=Y(KK)+OPT(KK)*AK
        IF (ABS(XP(K)).GT.Y(K)).LE.0.5) GO TO 18
        IF (XP(K).GT.Y(K)) GO TO 19
        OPT(K)=-1.
        GO TO 20
19 OPT(K)=1.
20 IF (K.EQ.2) GO TO 21
    KKK=K-2
    IF(OPT(K).NE.OPT(KK).AND.OPT(KK).NE.OPT(KKK)) GO TO21
    IF(OPT(K).NE.OPT(KK)) GO TO 22
```

```
IF (CHK.NE.1) GO TO 24
AK=1.
24 AK =AK+ABS(OPT(KK))
CHK=0.
GO TO 17
18 OPT(K)=0.
AK=2.
CHK=1.
GO TO 17
21 AK=1.
CHK=1.
GO TO 17
22 AK=ABS(AK-1.)
CHK=1.
GO TO 17
17 DEVIA=DEVIA+ABS(XP(KK)-Y(K))/(NN-1)
PRINT,DEVIA
PRINT 16 ,(XP(K),K=1,45)
PRINT 16 ,(Y(K),K=1,45)
XS(1)=0.
YS(1)=0.
DO 13 K=2, NN
KK=K-1
XS(K)=XP(KK)/8.
13 YS(K)=Y(K)/8.
IF (S.EQ.-1.) CALL PLOT (0.0,0.0,-3)
CALL AXIS (0.0,0.0,'K',-1,5.0,0.0,1.0,10.0)
CALL AXIS (0.0,-5.0,'X,Y',3,10.0,90.0,-40.0,8.0)
CALL PLOT (0.0,0.0,3)
CALL LINE (Q,XS,45,-1)
CALL PLOT (0.0,0.0,3)
CALL LINE (Q,YS,45,-1)
CALL PLOT (0.0,0.0,3)
CALL PLOT (7.0,0.0,-3)
```

```
      IF (S) 206,207,200
206 DO 201 K=2,NN
201 XP(K)=X(K)
      S=0.
      GO TO 202
207 DO 204 K=2,NN
204 XP(K)=XNKF(K)
      S=1.
      GO TO 202
202 CALL PLOT (0.0,0.0,-4)
      STOP
      END
```

```
SUBROUTINE SUBI (D,CC)
DIMENSION CC(3,3)
CC(1,1)=D
CC(2,2)=D
CC(3,3)=D
CC(1,2)=0.
CC(2,1)=0.
CC(3,1)=0.
CC(1,3)=0.
CC(2,3)=0.
CC(3,2)=0.
RETURN
END
```

**The vita has been removed from
the scanned document**

A PREDICTIVE ADAPTIVE DELTA MODULATOR

by

Yuh-tai Ju

(ABSTRACT)

A method is surveyed for telephone communication using a predictive adaptive delta modulator. This method is based on an estimation of the input waveform and an encoding of the signal into a digital sequence. The Kalman Filter does this estimation to filter out some of the noise, thus increasing the fidelity of the output to the original signal. The adaptive delta modulator does the encoding and allows the digital output to be reconstructed by a decoder which is identical to the feedback portion of the encoder.

In implementing the adaptive delta modulator, a bi-state quantizer and tri-state quantizer are presented for comparison. Since the granular region difficulties can be eliminated by the tri-state quantizer, the tri-state quantizer ADM provides a better stability.

The present design also consists of a predictor which is based on the theory of a Taylor series expansion in order to match the overload rate whenever the signal slope becomes too sharp. The results indicate that the present design is suitable for implementation when the incoming messages are highly correlated—implying rapid signal sampling.